Document Title:	Detection of Ignitable Liquid Residues in Fire Debris by Using Direct Analysis in RealTime Mass Spectrometry (DART-MS)
Author(s):	Mengliang Zhang, Ph.D., Ngee Sing Chong, Ph.D.
Document Number:	309916
Date Received:	December 2024
Award Number:	2020-DQ-BX-0003

Detection of Ignitable Liquid Residues in Fire Debris by Using Direct Analysis in Real-Time Mass Spectrometry (DART-MS)

AWARD NUMBER: 2020-DQ-BX-0003

Final Technical Report

Principal Investigator:

Mengliang Zhang, Ph.D.

Associate Professor, Department of Chemistry and Biochemistry, Ohio University

Athens, OH 45701

Co-Investigator:

Ngee Sing Chong, Ph.D.

Professor, Department of Chemistry, Middle Tennessee State University

Murfreesboro, TN 37132

Abstract

Identification of ignitable liquids (ILs) in fire debris evidence can be challenging and inconclusive, often due to the loss of signature volatile compounds. The detection of less-volatile compounds in IL residues holds significant forensic value in arson investigations, aiding in identifying or narrowing down potential ILs. These less-volatile compounds are relatively more stable and are, therefore, more likely to persist as reliable evidence in arson cases. The standard practice for analyzing IL residues in fire debris involves profiling volatile compounds through passive headspace extraction with activated charcoal (ASTM E1412) and subsequent GC/MS analysis (ASTM E1618). However, there has been limited research on methods for analyzing less-volatile IL residues in a forensic context despite the prevalence of such compounds—including glycol ethers, heavy hydrocarbons, and fuel additives—in various ILs. While the conventional GC/MS method remains the gold standard for IL analysis in forensic laboratories, it is limited in its ability to detect less-volatile compounds. This project leveraged the unique capabilities of DART-MS to detect less-volatile components in IL residues and applied multivariate statistical methods to enhance the discrimination of different ILs across various substrates and fire debris samples. Less-volatile marker compounds were identified, and extraction methods targeting these markers were developed. When solid-phase microextraction (SPME) was coupled with DART-MS, it enabled the reanalysis of fire debris evidence following activated charcoal strip extraction (ASTM E1412). This approach revealed less-volatile markers in IL residues, significantly enhancing the evidentiary value of the samples. Integrating chemometric approaches with GC/MS and DART-MS data further improved the classification of ILs, particularly for those with similar profiles when analyzed using only one technique. GC/MS demonstrated superior resolving power for detecting various volatile organic compounds in ILs, which is critical for distinguishing between different IL types. DART-MS provides complementary data on less-volatile chemicals, such as ion clusters for fuel additives, offering orthogonal insights that enhance the existing GC/MS methodology. The project resulted in scholarly outputs, including project reports, peer-reviewed articles, and conference presentations, thereby contributing to the advancement of forensic analytical techniques for detecting IL residues.

Table of Contents

Executive Summary

Purpose, Goals, and Objectives

This project was carried out in response to the need to address several of the OSAC research and development goals under the areas of 'Fire Debris & Explosives' and 'Fire & Explosion Investigation'. There are four major goals in this project:

- To determine the less-volatile/nonvolatile chemical fingerprinting profiles of ignitable liquids (IL) residues from fire debris samples by DART-MS.
- To develop optimum sample preparation procedures.
- To investigate the effects of various factors such as substrates, burning degrees, and water.
- To apply chemometric strategies to classify IL residues in fire debris.

To achieve these goals, the following tasks were accomplished:

1) Various ignitable liquids were screened using the DART-MS and GC/MS methods, and their profiles were compared and evaluated.
2) Weathered ignitable liquids were prepared under different conditions to study the variations of their DART-MS and GC/MS profiles, with an emphasis on the spectral profiles from the less volatile components.
3) Key characteristic less-volatile marker compounds for ignitable liquids (i.e., fuel additives in gasoline and polyethylene glycol in paint thinner) were identified.
4) Multiple sample preparation approaches were studied to extract the less volatile marker compounds of IL residues from substrates and debris, and the solid phase microextraction (SPME) method was developed to recover the IL residues.
5) A comparative evaluation of burning conditions, substrate types, and water effects on their chemical profiles was conducted.
6) Chemometric strategies were applied to classify IL liquid samples and IL residues in fire debris based on their DART-MS spectral and GC/MS chromatographic profiles.

Research Design, Methods, and Findings

Phase I: Study of pristine and weathered IL by DART-MS and GC/MS

Both DART-MS and GC/MS methods were developed for analyzing various ILs, including gasoline, paint thinner, Zippo lighter fluid, torch fuel, charcoal lighter fluid, kerosene, diesel, and Japan drier. These ILs were weathered at three different temperatures—30°C, 90°C, and 210°C—to varying extents, with weight loss ranging from 30% to 95%, and subsequently analyzed using both GC/MS and DART-MS. Additionally, fresh ILs such as lamp oil, lamp lighter, adhesive remover, belt conditioner, and fuel injector were analyzed using DART-MS. While the GC/MS TIC profiles showed significant variations influenced by weathering degree and temperature, the DART-MS spectral profiles exhibited greater resilience to the weathering process. The method for analysis of variance-principal component analysis (ANOVA-PCA) was applied to examine the variations in both GC/MS TIC and DART-MS spectral profiles, evaluating the qualitative and quantitative contributions of weathering degree and temperature to the total variance. Our findings indicate that DART-MS effectively distinguishes between different ILs under various weathering conditions. While it does not replace GC/MS for IL analysis, DART-MS serves as a valuable complementary method, enhancing and supplementing the capabilities of GC/MS in identifying ILs.

Phase II: Identification of less volatile marker compounds of IL by DART-MS

Various less-volatile compounds present in ILs were observed and identified. For instance, in gasoline samples, octadecanamide and polymeric fuel additive compounds were detected using DART-QTOF-MS. In paint thinner samples, glycol ether derivatives, such as polyethylene glycol (PEG), were identified by comparing the DART-MS spectra with PEG standards. Profiles based on these less-volatile marker compounds demonstrated consistency across fresh, lightly weathered, and even heavily weathered IL samples. This suggests that these compounds could serve as robust markers for detecting ILR, as they are more likely to persist after weathering or exposure to high temperatures, such as burns.

Phase III: Recovery and detection of less volatile marker compounds from substrates and debris

Three approaches were explored to recover the less volatile marker compounds from IL residues for the DART-MS analysis. **Thermal Desorption DART-MS**: This method involved direct analysis of substrates with IL residues using a temperature gradient (30°C to 600°C). However, the high temperatures required to desorb the marker compounds also pyrolyzed the substrate materials, causing interference in the mass spectra. **Sorbent Tube Extraction**: Various sorbent materials were tested, with Carbopack X selected for its relatively low background signal. After extraction, the sorbent tube was placed in a heating jacket-based online desorption system with N_2 flow, allowing the desorbed molecules to be directly analyzed by DART-MS. This method successfully detected polymeric compounds in fuel injector fluid samples. However, the extraction and desorption process was complex, making it impractical for routine forensic lab use. **Solid Phase Microextraction (SPME)**: SPME was optimized for extracting less-volatile marker compounds from gasoline and paint thinner samples. The SPME-DART-MS setup effectively analyzed ILR from substrates and fire debris matrices. The method demonstrated the ability to recover and detect volatile and less-volatile marker compounds. Optimization studies using second-order polynomial models indicated that high extraction temperatures (120–150°C) were necessary for less-volatile compounds. The characteristic ion patterns of gasoline residues in the low-to-mid mass range (< m/z 700) closely matched those of liquid samples directly analyzed by DART-MS. Desorption of ILR from the SPME fiber was achieved by exposing the fiber to the DART-MS helium gas stream at 400°C for 1 minute, with no carry-over detected. Additionally, this method was effective in reanalyzing debris samples previously subjected to traditional activated charcoal strip extraction (ASTM E1412 method), which could significantly enhance their evidentiary value.

Phase IV: Effects of substrate types, burning conditions, and water to IL detection by DART-MS

In ILR analysis, the substrate matrix often interferes with the identification of ignitable liquids used in arson crimes. Using SPME to extract liquid gasoline residues, followed by analysis with DART-MS, revealed characteristic ions corresponding to both volatile and less-volatile compounds. Similarly, SPME-DART-MS analysis of substrates and fire debris showed the presence of various ions indicative of gasoline residues. Gasoline residues on substrates such as paper, sand, wood, and fabric consistently exhibited low m/z ions across all sample replicates. Characteristic ions at *m/z* 93.5, 107.5, 121.5, 135.5, 284.5, 474.5, 530.5, and 586.5 were detected in all substrate samples, except for fabric, where *m/z* 530.5 was unresolved due to interference from polymeric backbones in the material. Higher mass ions, such as *m/z* 642.5 and 698.5, were not detected in most substrates. This is likely due to the decreased volatility of polymeric compounds with higher molar mass, which require more energy to overcome intermolecular forces and evaporate. Similar trends were observed in fire debris samples. Overall, the SPME-DART-MS analysis of substrates and fire debris consistently identified gasoline-related ions below *m/z* 700. Other factors, such as burning conditions and the effects of water, were also evaluated; however, the results were inconclusive. This work will continue in a subsequent project to address these challenges further.

Phase V: Application of statistical/chemometric strategies to classify IL liquid samples and IL residues in fire debris based on their DART-MS spectral and GC/MS chromatographic profiles

The receiver operating characteristic curve (ROC) analysis was used to select the optimum number of characteristic ions for gasoline identification. ROC was created by plotting the "sensitivity" to the "1-specificity" at various decision thresholds, defined by the number of characteristic ions for gasoline observed in the mass spectrum. For example, if the threshold was arbitrarily chosen to be four ions, the detection of four or more characteristic ions was determined as "identification," otherwise as "inconclusive." The sensitivity was obtained by dividing the sum of true positive outcomes by the total positive instances (or true positive rate). The "1-specificity" was calculated by dividing the sum of false positives by the total of negative instances (or false positive rate). The area under the curve (AUC) was derived from ROC analysis as an accuracy metric, for which values above 0.9 indicate a 'rather high' discrimination accuracy. When four characteristic ions were selected as the threshold, the true positive rate was 92.0%, and the true negative rate was 95.2%, which was considered optimal in this analysis (slightly favored the specificity to minimize the risk of wrongful convictions in arson cases). Based on this evaluation, the four most discriminative ions for gasoline identification were *m/*z 284.5, 474.5, 530.5, and 586.5.

Partial least squares discriminant analysis (PLS-DA) models were constructed by using GC/MS TIC and DART-MS spectral profiles with fresh and weathered IL, and the classification rates are 99.97 ± 0.02% and 99.80 ± 0.08%, respectively. The result indicates that both data representations could be used to distinguish the ILs. The paint thinner and Japan Drier are both medium petroleum distillates based on the National Center for Forensic Science classification scheme and have shown similar GC/MS TIC profiles in our study; therefore, they clustered close to each other. However, their profiles are distinctive in the DART-MS spectra: the signature polymeric glycol ether ions were not observed in the Japan Drier mass spectra; therefore, the paint thinner and Japan Drier were well separated on the PLS-DA score plot. On the other hand, the DART-MS spectra of the lighter fluid samples showed a distribution in the latent space near the paint thinner samples, but the GC/MS TIC profiles of the lighter fluid were different from those of the paint thinner samples. In summary, both GC/MS TIC and DART-MS data produce discriminative data profiles for IL classification, and DART-MS can complement the existing GC/MS method for identifying ILs.

Conclusions

The overall conclusions of this study are as follows:

- Less-volatile compounds are abundant in ignitable liquids (IL) but are often overlooked in traditional GC/MS analysis.
- DART-MS can effectively identify these less-volatile marker compounds in IL residues, offering complementary information to GC/MS.
- Coupling SPME with DART-MS enables the reanalysis of fire debris evidence following activated charcoal strip extraction (ASTM E1412 method), revealing less-volatile markers that could significantly enhance evidentiary value.
- Integrating chemometric approaches with GC/MS and DART-MS data improves the classification of ILs, particularly for those with similar profiles when analyzed by a single technique.

Implications for Criminal Justice Policy and Practice

Identifying IL in fire debris evidence can be challenging and inconclusive, often due to the loss of signature volatile compounds. Detecting less-volatile compounds in IL residues holds significant forensic value in arson investigations, helping to identify or narrow down potential ILs. While the conventional GC/MS method remains the gold standard for IL analysis in forensic laboratories, it is limited in its ability to detect less-volatile compounds. Our research provides the first comprehensive dataset for analyzing less-volatile components of IL in fire debris samples, offering new insights into fire debris evidence collected from crime scenes. Since less-volatile compounds are more likely to persist in samples after the extraction of volatile components through standard methods (e.g., ASTM E1412), the DART-MS method can be employed to reanalyze fire debris evidence following the application of current standard practices (e.g., ASTM E1412 and E1618). This complementary DART-MS data enhances the information obtained from conventional

GC/MS analysis. Additionally, this project serves as a case study, demonstrating how the DART-MS technique can be applied to analyze various other ignitable liquids. Although DART-MS is increasingly adopted in crime labs nationwide, its primary use has been for drug screening. Our research expands the instrument's capabilities, showcasing its potential for high-throughput screening in arson investigations. The results of this study contribute not only to the forensic science literature but also to improving the interpretation of arson evidence, providing a valuable supplement to current forensic practices.

Impact

This project offers valuable opportunities for the technical training of future forensic scientists through hands-on laboratory and research experience. The MTSU Forensic Science program requires students to complete internships in forensic laboratories to fulfill the B.S. in Forensic Science degree requirements. However, only about 30% of forensic science majors annually secure internships at agencies such as the Tennessee Bureau of Investigation (TBI), Nashville Metro Police Crime Laboratory, National Institute of Standards and Technology, and Aegis Sciences Corporation. This project has created three additional opportunities that fulfill the internship requirement. Students participating in this research receive training in lab techniques pertinent to fire-related crime investigations, forensic testing protocols, statistical quality assurance, and quality control for laboratory data. They also develop soft skills in teamwork, scientific communication, and best practices for maintaining both traditional and electronic lab notebooks. These experiences prepare students for competitive internships and job opportunities in the field.

Three undergraduate students have contributed to this project. Two of them used their research experience to complete their honors thesis requirement for the B.S. in Forensic Science degree. One was hired as a chemist in August 2023 by the TBI Forensic Services Division, joining the Microanalysis Team. The other entered the forensic toxicology graduate program at Texas Tech University in Fall 2024. The third undergraduate student earned course credit through their involvement and now works as a researcher at Georgia State University after graduating from MTSU.

A Ph.D. student supported by this project is also conducting her doctoral research based on this work. She has served as the first author of two journal publications in Forensic Chemistry and is the primary author of several national conference presentations.

Dissemination of Research Findings

The research team has actively disseminated the findings from this project through journal publications and conference presentations. The project has resulted in two journal publications in Forensic Chemistry and 15 presentations at national conferences.

- *Journal publications*

  [1] Perna, S., Dedicatoria, B., Chong, N.S., Zhang, M., ‘GC/MS and DART-MS as Complementary Methods for Investigating the Effects of Weathering on Chemical Profiles of Ignitable Liquids: A Case Study for Paint Thinner,’ *Forensic Chemistry*, **2023**, 33, 100478.

  [2] Perna, S., B., Chong, N.S., Zhang, M., ‘Recovery and detection of ignitable liquid residues from the substrates by solid phase microextraction - direct analysis in real time mass spectrometry,’ *Forensic Chemistry*, **2024**, 41, 100611.

- *Other publications, conference papers, and presentations.*

  [1] Perna, S., Chong, N.S., Zhang, M., ‘Comparison of Weathering Profiles of Ignitable Liquids by Gas Chromatography-Mass Spectrometry and Direct Analysis in Real-Time Mass Spectrometry.’ The American Society for Mass Spectrometry Annual Conference 2021, Philadelphia, PA. Nov **2021**. (Poster)

  [2] Boyce, R., Perna, S., Zhang, M., Chong, N.S., ‘Use of weathered hydrocarbon data from FTIR, Raman, and GC/MS analysis to identify different ignitable liquids and estimate their degree of weathering.’ Southeast Regional Meeting of American Chemical Society (SERMACS) 2021, Birmingham, Alabama, Nov **2021**. (Poster)

  [3] Perna, S., Chong, N.S., Zhang, M., ‘A Comparison of Weathering Profiles of Ignitable Liquids (ILs) by Gas Chromatography/Mass Spectrometry (GC/MS) and Direct Analysis in Real-Time Mass Spectrometry (DART-MS),’ AAFS 2022 Conference. Seattle, WA. Feb **2022**. (Poster)

[4] Zhang, M., Perna, S., Dedicatoria, B., Chong, N.S., ‘Comparison of Weathering Profiles of Ignitable Liquids by GC/MS and DART-MS,’ 2022 NIJ Forensic Science R&D Symposium. Mar **2022**. (Poster, virtual)

[5] Dedicatoria, B., Perna, S., Chong, N.S., Zhang, M., ‘Multivariate Factor Analysis to Study the Variation of the GC/MS Profiles of Ignitable Liquids During the Weathering Process,’ FACSS SciX 2022 Conference. Covington, KY. Oct **2022**. (Poster)

[6]. Zhang, M., Perna, S., Dedicatoria, B., Chong, N.S., ‘Comparative Evaluation of Ignitable Liquid Residue Detection by GC/MS and DART-MS.’ 6th NIJ Forensic R&D Symposium PITTCON. Philadelphia, PA. Mar **2023**. (Oral)

[7]. Zhang, M., Perna, S., Chong, N.S., ‘Analysis of Less Volatile Components in Ignitable Liquids by Direct Analysis in Real Time Mass Spectrometry and Versatile Sampling Strategy.’ NIJ Forensic Science R&D Symposium Poster Session. Orlando, FL. Feb **2023**. (Poster)

[8]. Perna, S., Chong, N.S., Zhang, M., ‘The Unique Capability of DART-MS for the Detection of Less Volatile Components in Ignitable Liquids.’ AAFS 2023 Conference. Orlando, FL. Feb **2023**. (Poster)

[9]. Perna, S., Delicatoria, B., Chong, N.S., Zhang, M., ‘Identification of Ignitable Liquids by Gas Chromatography-Mass Spectrometry and Direct Analysis in Real-Time-Mass Spectrometry via Their Marker Compounds,’ The American Society for Mass Spectrometry Annual Conference 2023. Houston, TX. June **2023**. (Poster)

[10]. Zhang, M., Perna, S., Chong, N.S., ‘Ignitable Liquid Analysis by DART-MS and Chemometrics,’ FACSS SciX 2023 Conference. Sparks, NV. Oct **2023**. (Oral)

[11]. Perna, S., Bascou, V., Chong, N.S., Zhang, M., ‘Recovery and analysis of both volatile and less-volatile compounds from ignitable liquid residues on substrates/debris by SPME-DART-MS,’ NIJ Forensic Science R&D Symposium Poster Session at AAFS 2024 Conference. Denver, CO. Feb **2024**.

[12]. Perna, S., Bascou, V., Chong, N.S., Zhang, M., ‘Detection of ignitable liquid residues using solid-phase microextraction direct analysis in real-time mass spectrometry (SPME-DART-MS),’ 7th NIJ Forensic R&D Symposium PITTCON. San Diego, CA. Feb **2024**.

[13]. Perna, S., Bascou, V., Chong, N.S., Zhang, M., 'Solid phase microextraction coupled direct analysis in real-time mass spectrometry (SPME-DART-MS) for the ignitable liquid

residue analysis,' The American Society for Mass Spectrometry Annual Conference 2024. Anaheim, CA. Jun **2024**.

[14]. Zhang, M., Beyond Volatile Organic Compounds (VOC) for Ignitable Liquid Residue Detection: Comparison of Results Using DART-MS and GC/MS,' he 21st Annual Ohio Mass Spectrometry Symposium. Columbus, OH. Oct **2024**.

[15]. Zhang, M., Perna, S., Chong, N.S., Chemical Fingerprint of Ignitable Liquid Residues by DART-MS: More Than Volatile Organic Compounds (VOC),' Eastern Analytical Symposium and Exposition. Plainsboro, NJ. Nov **2024**.

Main Body

Section 1. GC/MS and DART-MS as Complementary Methods for Investigating the Effects of Weathering on Chemical Profiles of Ignitable Liquids: A Case Study for Paint Thinner

1.1 Introduction

Arson is the crime of the deliberate act of setting fire to property (e.g. house, building, ship, or forest) or one's insured property with the intent to defraud the insurers [1]. Arson hurts society through property damage and loss of life and creates a sense of insecurity in the community. The arson investigation is complicated because much of the evidence is destroyed or altered by the fire itself, and additionally, the firefighters could have caused the contamination or alteration of the fire scene. Ignitable liquids (ILs) are commonly used as accelerants in arson attacks to initiate and intensify fires [2]. The identification and accurate determination of the ignitable liquid residues (ILR) are critical to providing an evidentiary link between the arson and the suspect. The most commonly used ILs in arsons are gasoline, kerosene, charcoal lighter fluid, paint thinner, and other less common fuels [3]. Hence, forensic investigators are tasked to examine the ILR samples for their identification and characterization proactively.

For the IL analysis, techniques such as nuclear magnetic resonance spectroscopy (^{1}H and ^{13}C), fluorescence spectroscopy, near-infrared spectroscopy, and gas chromatography have been applied [4-8]. Among these, in forensic labs, gas chromatography coupled with mass spectrometry (GC/MS) is the most widely used tool to analyze IL and ILR samples. For the fire debris analysis, the American Society for Testing and Materials (ASTM) E1618 has set analytical guidelines for the GC/MS identification and classification of the unknown ILR from fire debris [9]. This process involves comparing the GC/MS data from the unknown and reference samples based on their total ion chromatograms (TIC), extracted ion chromatograms, target compounds, or a combination thereof. Other GC/MS data representations, including the total ion spectrum (TIS) [10], selected mass spectral ions [11], and two-way GC-MS data [12], were also applied in studying the IL profiles when combined with the chemometric methods. The GC/MS is capable of analyzing the volatile components in the ILR; however, it is critical to understand the non-volatile or less volatile components for the identification of the IL. At the same time, the study of less volatile marker compounds in IL and the factors affecting their distribution also provides valuable information. For example, in gasoline and diesel, non-volatile detergents like polyisobutylene, succinimides, and polyether amines are added to reduce the formation of deposits in the engine parts, and these compounds can act as marker compounds for the fuel brands [13, 14]. In recent years, direct analysis in real-time mass spectrometry (DART-MS) has emerged as a powerful ambient ionization mass spectrometry technique to analyze IL and ILR [15, 16]. DART-MS is becoming more available in forensic laboratories and has been used to analyze various forensic samples [17]. It is a simple and rapid analytical method that utilizes metastable gas atoms to desorb and ionize the compounds of interest. Some of the DART-MS advantages this method offers are minimal sample preparation, good analytical sensitivity, and the capability to analyze volatile and non-volatile compounds. DART-MS can analyze a variety of sample matrices via sample introduction modules such as QuickStrip^{TM}, thermal desorption, and a tweezer module [18].

When the ILs are exposed to air, the more volatile chemical components will evaporate preferentially; this process is called weathering. As the chemical components in the ILs have different boiling points or vapor pressures, the weathering is not uniform, and it alters the relative quantities of constituents in the mixture. Therefore, comparing weathered to non-weathered ILs becomes difficult for forensic chemists [19]. In the standard procedure, the IL collected at the crime scene is compared with the suspected weathered reference IL profile to improve the accuracy or reliability of IL identification. Further study of the factors during the IL weathering process can benefit the criminalist in analyzing fire debris for arson. The weathering effects on IL samples have been studied using different approaches; for example, Willis *et al.* have quantitatively compared the weathering residues of artificial gasoline at elevated and room temperatures by the thermodynamic model approach [19]. Bruno *et al.* have studied IL weathering by the advanced distillation curve method using a mathematical model to predict the evaporation patterns of the suspected IL in relation to the temperature, and the method could generate the expected evaporation pattern of the less common ILs found at the crime scene [20]. The chemometric approaches could be useful in understanding the weathering process of IL. In another study by Sigman *et al.*, the weathering data obtained from the GC/MS analysis was visualized and classified by covariance mapping. This method helped categorize the matrix-contaminated post-burn samples into lightly or heavily weathered samples [21]. Since both weathering extent (or degree) and temperature affect the concentrations of compounds in the IL samples, the multivariate factor analysis methods, such as analysis of variance-principal component analysis (ANOVA-PCA), could be an effective approach for studying their impact on the chemical profiles. Firstly introduced by Harrington *et al.* to discover biomarkers in the proteomic study [22], ANOVA-PCA has been applied to classify gasoline samples based on their brands and sample collection periods [14]. This method separates the variation of the experimental hypothesis from other potentially confounding sources of variation, and it is ideal for investigating the problems with multi-factorial variation due to the weathering degree and temperature effects in the ILR weathering process. ANOVA-PCA provides an effective means to interpret the impact of each experimental factor on the data profiles and assist in identifying the potential marker compounds corresponding to the factors.

In this section, our objectives were to investigate the chemical profile changes of a common but less studied IL, paint thinner, during the weathering process, compare the results of DART-MS analysis to data from the conventional GC/MS, apply the chemometric methods such as ANOVA-PCA to better understand the impact of weathering degree and temperature factors in the weathering process, and identify the potential marker compounds for the detection of ILR.

Table 1. Details of ILs used in this study

IL Type	Brand	Product #	Volume (mL)	Classification*	Abbreviation
Paint Thinner	Klean-Strip®	QKPT943	946	MPD	PT
Lighter Fluid	Zippo	132012-M	118	LPD	LF
Japan Drier	Klean-Strip®	JD-40	946	MPD	JD
Torch Fuel	TIKI BiteFighter	1215090	1890	HPD	TF
Gasoline	Speedway	NA	NA	GAS	GAS
Paint Thinner	Klean-Strip®	QKPT943	946	MPD	KS plastic bottle PT
Paint Thinner	Klean-Strip®	QKPT94003	946	MPD	KS blue metal bottle PT
Paint Thinner	Klean-Strip®	PT-1K-1675-782	946	MPD	KS white metal bottle PT
Paint Thinner	Klean-Strip®	Barco-03271	473	MPD	KS Barco PT
Paint Thinner	Crown	CPTM4-PS1106	946	MPD	Crown PT

*HPD, heavy petroleum distillates; LPD, light petroleum distillates; MPD, medium petroleum distillates; GAS, gasoline

1.2 Materials and Methods

1.2.1 Ignitable liquid sample collection

Ignitable liquid samples, including Klean-Strip® Paint Thinner (1 quart), Zippo lighter fluid (118 mL), Klean-Strip® Japan Drier (0.473 L), and TIKI BiteFighter torch fuel (1.89 L), were purchased from the local Walmart stores. Gasoline with octane number 87 was acquired from Speedway fuel stations. Another set of five different paint thinner products was collected from various local suppliers. All the ILs were classified into one of the ASTM classes based on their GC/MS data, and details of ILs used in this study are available in Table 1. Reagent-grade chloroform was purchased from Fisher Scientific (Pittsburgh, PA).

1.2.2 Weathered IL sample preparation

Aliquots of 2-18 mL of IL samples were weathered in glass vials at different temperatures, including 28 °C, 90 °C, and 210 °C, to varying degrees of weathering at 30-99% mass reduction before being analyzed. After weathering, the vials were capped and stored at −4 °C until the analysis.

1.2.3 DART-MS and GC/MS

For DART experiments, the DART ion source (IonSense, Inc., Saugus, MA) was coupled to a Thermo LTQ XL mass spectrometer (Thermo Scientific, San Jose, CA), and the ionization gas used was helium. The DART gas heater was set to 350 °C, and the mass spectra were collected in an *m/z* range of 50-1000 in the positive ion mode. An automated sample introduction apparatus with Linear Rail Enclosure that holds disposable QuickStrip^{TM} sample cards was used to analyze the IL samples on DART-MS. The preloaded QuickStrip method, as described in the publication of Barnett *et al.* [14], was used in this study. A 5 µL IL sample was spotted on the card after a ten-fold dilution of the sample in chloroform. The triplicate samples were spotted in each of the twelve slots of the QuickStrip™ sample card, with blanks in between each set of triplicates for background subtraction. In between runs, the QuickStrip™ module was cleaned using methanol to prevent the carryover signals from the previous run to the next run.

For the GC/MS analysis, 20 µL of the sample was added to 1 mL of chloroform, followed by an injection of 1 µL with a split ratio of 1:50. The GC injector temperature was at 250 °C, and the analytes were separated on a ZB-35HT, 30 m × 0.25 mm I.D. capillary column chemically bonded with 35% diphenyl/65% dimethyl polysiloxane at 0.25 µm film thickness (Phenomenex, Torrance, CA). A constant helium flow of 1 mL/min was used. The GC column temperature program had the initial oven temperature at 50 °C with an initial hold for 3 min followed by a ramp rate of 10 °C /min to reach 310 °C with a final hold for 4 min. The ion source temperature was 250 °C, and the interface temperature was 310 °C. The full scan mode was selected for the mass spectrometer, and the scan range was from *m/z* 30-350.

1.2.4 Data analysis

The GC/MS data were acquired as QGD files and then converted to the network common document format (CDF) with the Shimadzu GCMSsolution software (Shimadzu Corp., Kyoto, Japan). The CDF files were read directly into MATLAB R2021a (MathWorks Inc., Natick, MA) using the "*netcdf*" function.

Correlation-optimized time warping (COW) has been introduced previously as one of the numerous pretreatment methods to overcome the misalignment problems in chromatograms.[24] The COW method first segments both the sample chromatogram and reference chromatogram, and then a dynamic programming algorithm is applied to optimize the interpolation of the sample segments. The optimum correlation of each segment between the sample and reference chromatograms is combined to provide a global optimum of retention time alignment.[25] The reference chromatogram is required to implement the COW method, and usually, the chromatogram with the highest correlation coefficient should be selected. In this work, the peak distributions in TIC chromatograms of IL varied dramatically due to the difference in weathering degrees. Therefore, the average chromatogram of the samples from all weathering degrees was used as a reference chromatogram, which includes almost all the observed peaks in TICs, so that the retention time drift of all samples could be corrected regardless of weathering degrees. The number of segments for COW is 25, and the maximum range or degree of warping in the segment is 5.

For DART-MS data, the average mass spectrum of 60 scans (0.17 min) for each sample was exported to Excel with Xcalibur 2.1 software (Thermo Scientific, Waltham, MA) after the background spectrum was subtracted. The data sets were binned by mass-to-charge ratios from 50 to 1000 Th with 0.5 Th increments.

The statistical and chemometric analysis was conducted using MATLAB R2021a (MathWorks Inc., Natick, MA) with the PLS toolbox (Eigenvector Research, Inc., Manson, WA).

Both GC/MS TIC and DART-MS spectral profiles were normalized to unit vector length [33, 34] before further PCA or partial least squares discriminant analysis (PLS-DA).

1.3 Results and Discussion

1.3.1 GC/MS Profiles for Paint Thinner Samples

TIC chromatogram is a common and convenient approach for the visualization and comparison of IL profiles, and chemometrics has been widely used to classify ILs based on the TIC of GC/MS data sets [22, 23]. However, the run-to-run retention time drifts in TIC chromatograms are unavoidable, and the variations, if not corrected, would undermine the effectiveness of the multivariate models. The retention time variation among paint thinner samples is shown in Figure 1A, in which retention time drift among different samples occurs in the entire GC program. After the COW alignment, the retention time distribution of each peak cluster is significantly narrower (Figure 1B). The benefit of COW alignment can also be visualized in the plot of the PCA scores. Figure 2A shows that the TIC of all weathered paint thinner data sets is not well clustered based on the weathering degree, especially for the 70% weathered samples. The retention time alignment approach notably increases the similarity among chromatograms of the same weathering degree in the PCA score plot (Figure 2B), and the separation of clusters can be better defined. According to Figure 2, it is also noted that the samples with different weathering degrees are primarily separated on PC1 (*i.e.*, 30-70% weathered samples vs. 90-95% weathered samples), and the samples with the same weathering degree have different PC2 scores due to the weathering temperature effect. For example, the samples evaporated at room temperature often have more positive PC2 scores than those evaporated at 90 or 210 °C. The results indicate both weathering degree and temperature affect the paint thinner GC/MS TIC profiles. Though the alignment algorithms have shown effectiveness in minimizing the variations caused by the retention time drifts, their practical applications have some challenges. For example, the chemometric models are usually established first from known data sets (i.e., training set) and then applied to unknown samples (i.e., prediction set). The training and prediction data sets may have to be treated separately. One approach is to align both the training and prediction data sets to the average of the training set [26]. This can be problematic when the presence of substrates, microbial degradation, and other environmental factors cause the retention time shifts in the TIC of the unknown samples. The issue can become more significant for experimental parameter changes (e.g., a new GC column installed) and interlaboratory TIC comparison. Therefore, in the forensic laboratory, comparing TIC is the critical first step in data analysis, and the extracted ion profiling and target compound analyses are necessary for interpreting results [9].

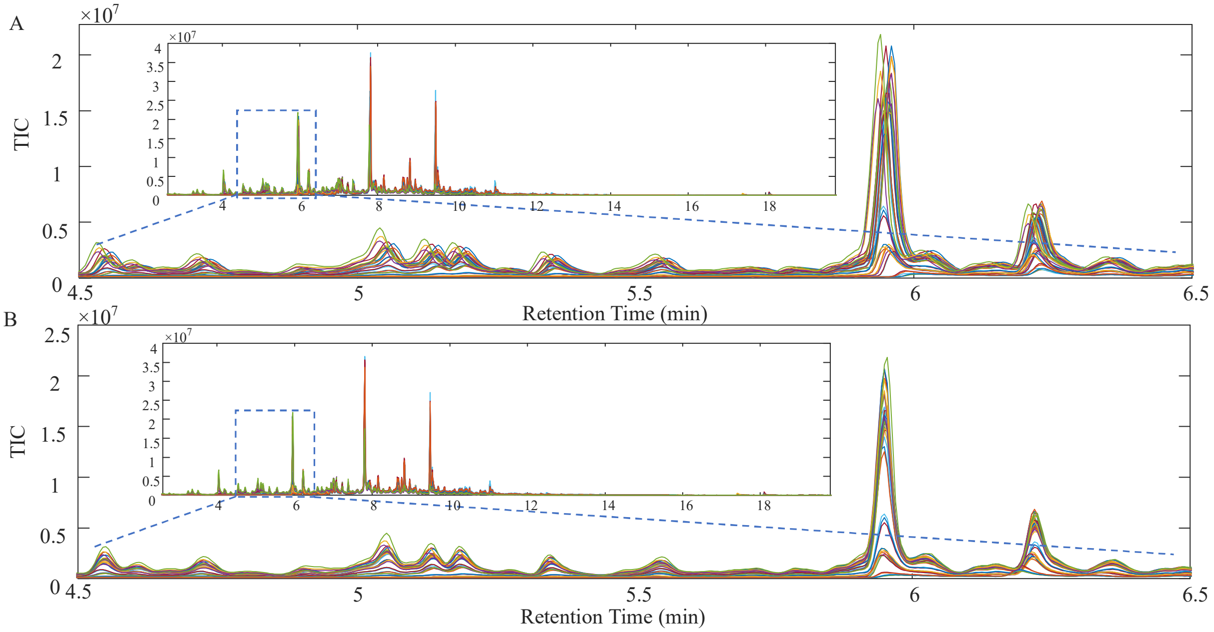

Figure 1. GC/MS total ion current (TIC) chromatograms of 45 paint thinner samples in the retention time windows of 4.5-6.5 min are shown in (A) without retention time alignment and (B) after retention time alignment. The entire TIC chromatograms are provided as inserts.

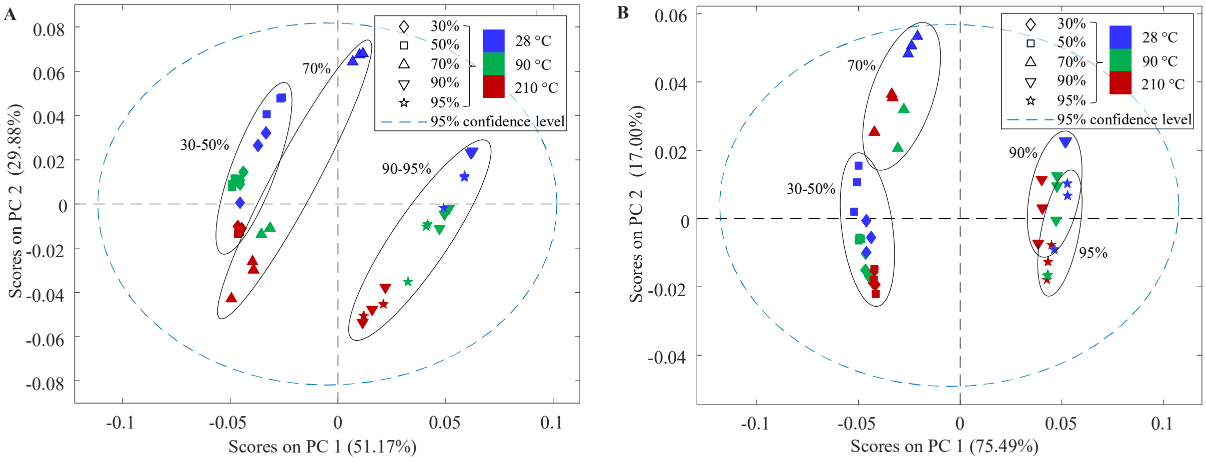

Figure 2. Principal component analysis score plots for paint thinner GC/MS TIC data before (A) and after (B) COW retention time alignment. The percent variance spanned by the principal components is given in parentheses with the absolute variance. Data are normalized to the unit

vector before performing PCA. Note the oval shapes are for labeling purposes only and have no statistical meanings.

The TIC pattern shift shown in Figure 3, specifically for paint thinner, is similar to the weathering pattern shown by any ignitable liquid composed of many chemical components of different volatilities [3]. In the weathering process, two factors, including weathering degree and temperature, were found to significantly affect the chemical profiles of ILs. For example, various studies have investigated the effects of weathering on the relative distribution of the chemical components of gasoline and have found that both the extent of weathering and weathering temperature influence the chemical profiles of gasoline. Overall, the fractions of more volatile components, such as toluene, decrease with the extent of weathering, whereas the fractions of less volatile components, such as 1,2,4-trimethylbenzene and naphthalene, increase due to the more significant loss of the more volatile components [19]. In addition, the elevated weathering temperature (e.g., 210 °C), especially at higher weathering degrees of 90% or 95%, leads to relatively high fractions of the volatile components (e.g., Peak #2 for 3-ethyl-5-methyl heptane) as a result of a greater relative increase in the vapor pressures of the less volatile components (e.g., Peak #7 for dodecane with a boiling point of 216 °C) in the mixture than the more volatile components [27, 28]. In our paint thinner result, nonane (Peak # 1 in Figure 3) was the third or fourth tallest peak in the TIC profiles for fresh samples and lower-intensity peak for 30% and 50% weathered samples but became non-detectable in the more heavily weathered samples (e.g., 70%, 90%, and 95% weathered samples). On the contrary, dodecane (Peak # 7 in Figure 3) was shown as a minor peak in the fresh and lightly weathered samples (i.e., <70% weathered samples) but was one of the major peaks in the heavily weathered samples. This result agrees with the general trend for chemical profile variations in weathered ILR samples based on the volatilities (e.g., 4.45 mm Hg and 0.135 mm Hg at 25 °C for nonane and dodecane, respectively, based on data from PubChem). The temperature effect on the variations of the TIC profiles is less significant compared with the weathering degree effect, but it was noticeable that the relative intensity of the volatile compounds such as 3-ethyl-5-methyl heptane (Peak #2 in Figure 3) was higher in the highly weathered samples treated under the elevated temperature (e.g., 90% or 95% weathered samples prepared under 210 °C). Therefore, both weathering degree and weathering temperature factors contributed to the variations of the TIC profiles for paint thinner samples, which results in additional complexity for distinguishing paint thinner residues from other ILRs.

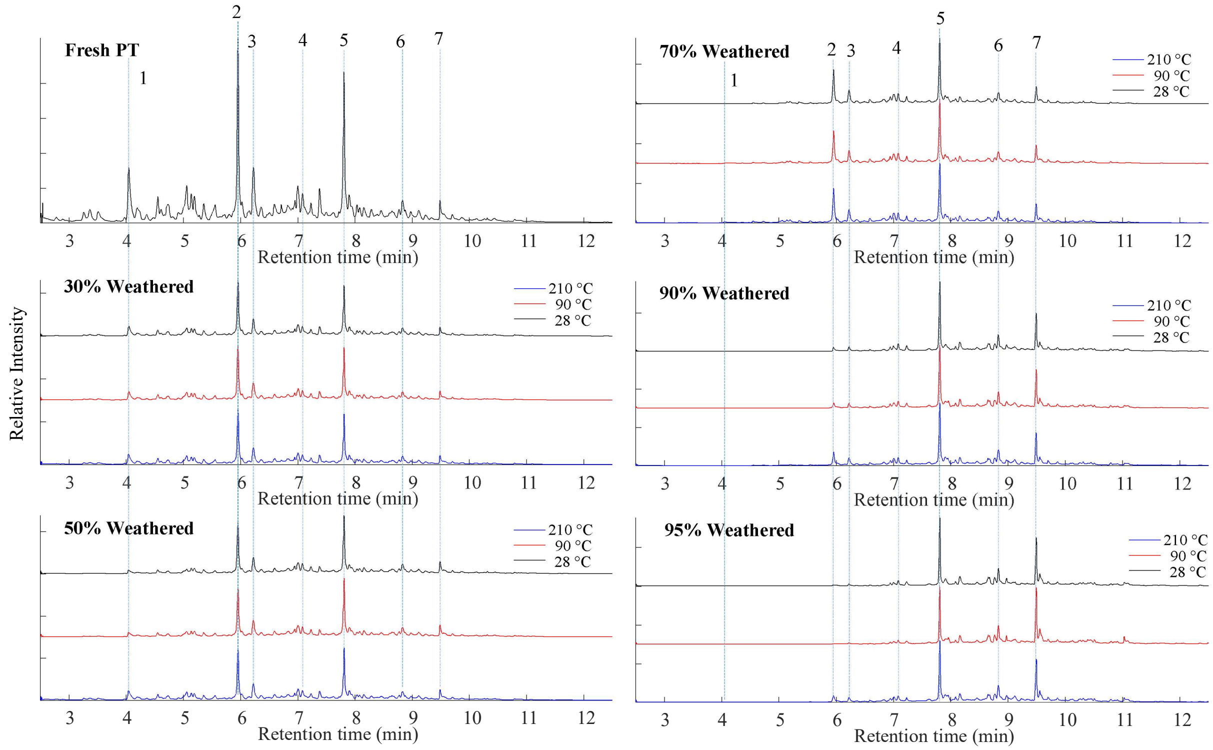

Figure 3. TIC chromatograms for fresh and weathered paint thinner samples from GC/MS analysis. Samples were weathered at different temperatures (i.e., black line for room temperature, red line for 90 °C, and blue line for 210 °C). Each TIC represents the average of three replicated chromatograms. Compounds identified from the labeled peaks: 1. Nonane; 2. 3-ethyl-5-methylheptane; 3. 4-methyldecane; 4. 1,2,4-trimethylbenzene; 5. Undecane; 6. 2-propyl-1-heptanol; 7. Dodecane.

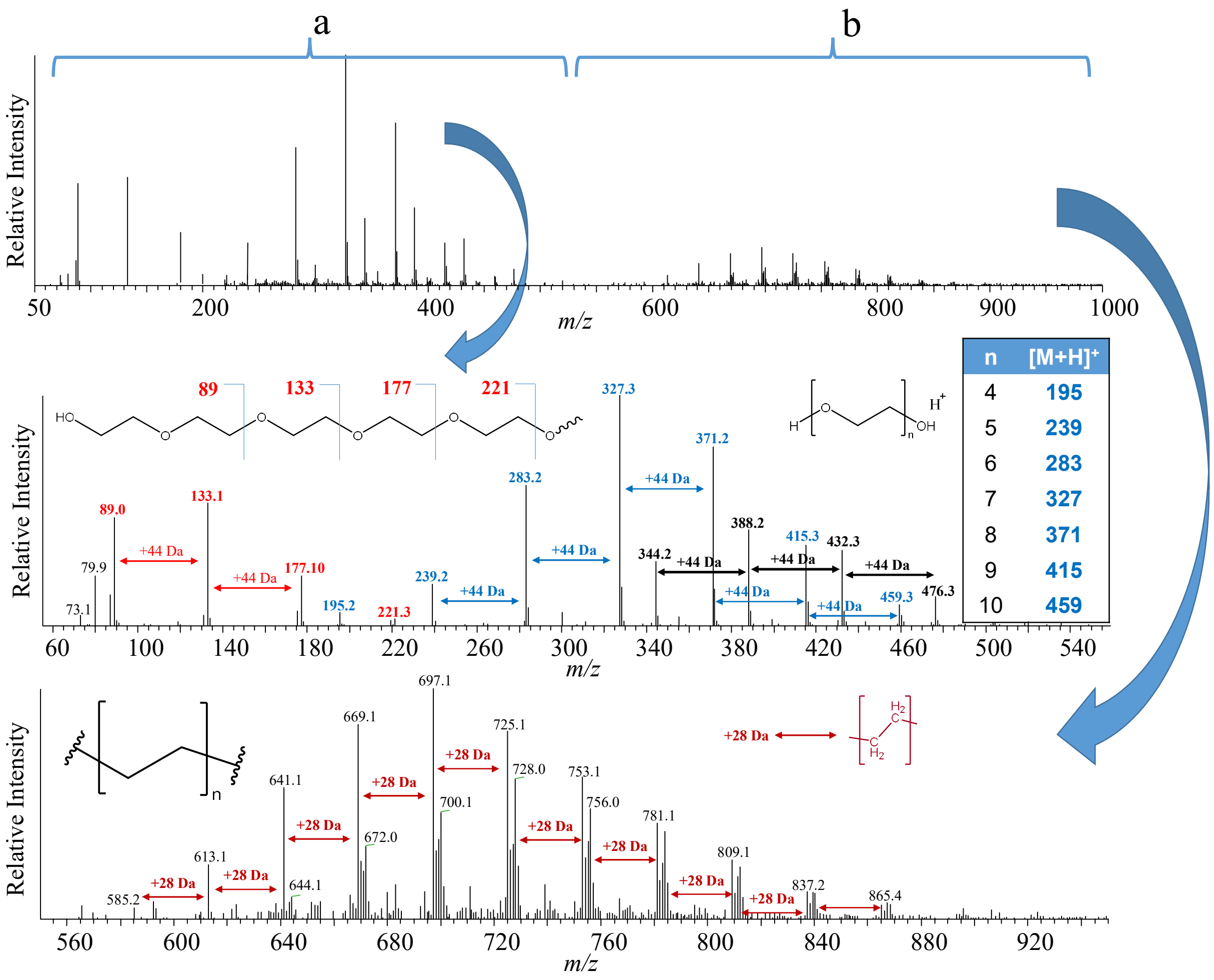

Figure 4. A typical DART-MS spectrum for paint thinner sample and magnified windows for Regions a and b. For Region a, the ions denoted in red font were tentatively attributed to the fragmentations of PEG. Blue arrows separate the protonated forms of PEG, and the black arrows represent the ammoniated forms of PEG. For Region b, the ions were tentatively attributed to the fragmentations of polymeric compounds with alkyl chains.

1.3.2 DART-MS Profiles for Paint Thinner

An example of a paint thinner DART-MS spectrum after background subtraction is shown in Figure 4. The peaks in the MS spectrum can be arbitrarily divided into two groups: *m/z* 50-550 in the Region (a) and *m/z* 550-1000 in the Region (b). There are three ion series in the mass spectral Region (a) of paint thinner samples separated by repeating units of 44 Da, which correspond to the ethylene oxide ($-O-CH_2-CH_2-$, 44.02621 Da) moiety. To the best of our knowledge, reports on analyzing glycol ethers by DART-MS are rare. The glycol ethers based on the propylene glycol were detected in E-cigarette liquids[29] and condom lubricants[30], but the ion clusters do not match those observed in our study. In addition, our ion series are consistent with the ethers of ethylene glycol analyzed by different mass spectrometric methods in other publications. For example, the polyethylene glycol (PEG) from an ethylene oxide with four monomers to 10 monomers was separated on a reversed-phase C8 HPLC column followed by the electrospray ionization mass spectrometry (ESI-MS) detection, and ion series of *m/z* 195.1228, 239.1489, 283.1752, 327.2018, 371.2284, 415.2542, and 459.2801 were identified as the protonated ions of these PEG compounds, respectively[31]. A similar ion pattern for PEG was also observed as background signals for the nanoLC-MS-based proteomic studies, and the ammoniated form of PEG ions (i.e., $H\text{-}[O\text{-}CH_2\text{-}CH_2]_n\text{-}OH + NH_4^+$) were also present[32], which is consistent with the mass spectra observed in Figure 4. Another ion series in the low mass range (e.g., *m/z* 89, 133, 177, and 221, red in Figure 3) of our DART-MS spectrum agreed with the signature fragmentation patterns of the low molecular weight PEG oligomers from multiple ionization sources, such as electron ionization MS (EI-MS)[33], ESI-MS/MS[34, 35], and isobutene chemical ionization MS/MS (CI-MS/MS)[36]. DART ionization mechanism in positive mode is mainly based on the ionization of atmospheric water via the metastable gaseous plasma followed by the charge transfer from the protonated water clusters to the analytes, and it is considered a 'soft' process with predominantly protonated molecules shown in the mass spectrum; however, in-source fragmentation or pyrolysis could be induced for some molecules, especially when the high DART gas heater temperature applies [37]. Therefore, the red ion series in Region (a) of Figure 4 could be formed by the fragmentation of the ethylene glycol compounds. The results from comparing the DART-MS spectrum and the published literature support the tentative identification of the mixture of ethylene glycol ethers in the paint thinner samples. In addition, a PEG 200 reference solution was analyzed by QuickStrip DART-MS and the mass spectrum is shown in Figure 5. The major ions in the DART-MS spectra of the paint thinner and PEG 200 samples are in close agreement with each other, though the relative abundances vary. The higher intensities for low-mass ions in the paint thinner spectrum indicate the compounds with lower molecular weights are the more dominant types of ethylene glycol ethers in the sample. Glycol ethers have been widely used in paints and cleaners [38, 39], and ethylene glycol and its polymer, PEG, can be found in many consumer products, such as cosmetics, cleaning agents, and inks [40, 41]. The presence and detection of ethylene glycol ethers in IL can be significant for forensic arson investigation because these compounds are less volatile and tend to be retained in the IL residues. For example, the boiling point for diethylene glycol is 246 °C with a vapor pressure of 5.7×10^{-3} mmHg, and the boiling point increases as the polymerization extent of ethylene oxide increases [42]. Our work is the first study to report the potential use of glycol ethers for IL identification. Another ion series in the mass spectral Region (b) of paint thinner samples was also observed in Figure 4, which were separated by repeating units of 28 Da, indicating the presence of polymeric compounds with various alkyl chain lengths (−CH2−CH2−, 28.0313 Da). Though the identity of the compounds cannot be confirmed, they are considered to be less volatile due to the high molecular weights (>580 Da) and polymeric nature, and together with ethylene glycol ethers, they could be used as the marker compounds for identifying paint thinners.

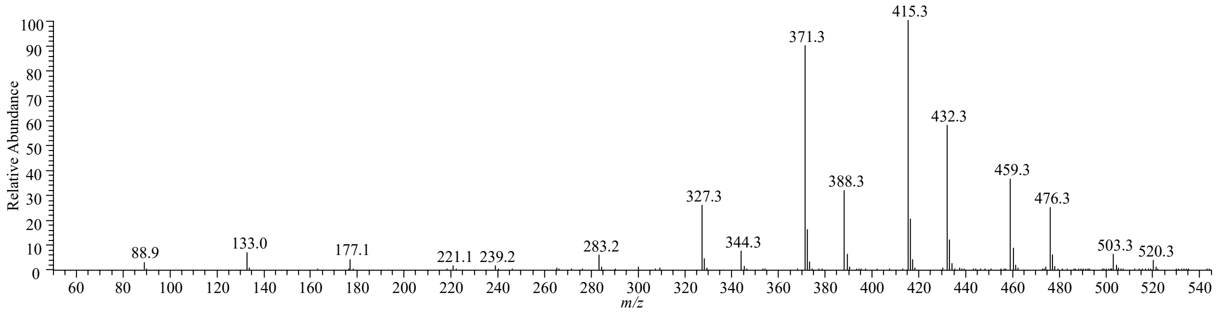

Figure 5. DART-MS spectrum for PEG 200.

The DART-MS spectra for the weathered paint thinner samples are shown in Figure 6. The DART-MS spectral profiles in Region (a) have a great similarity among the samples prepared under different weathering degrees and weathering temperatures, and the glycol ether relevant ions are dominant in the spectra of all samples. It is worth mentioning that although the glycol ether polymeric cluster peaks are the dominant ions in all the DART-MS spectra, their absolute concentrations in the paint thinner samples cannot be determined because the non-polar hydrocarbons, including alkanes and aromatics in the paint thinner, do not produce quantifiable ions in the DART ion source. Furthermore, the ionization efficiencies of different classes of polymeric components (e.g., ethylene glycol ethers and polymers with alkyl chains) are likely different and are susceptible to change due to experimental parameters such as helium flowrate and sample position relative to the skimmer sampling interface. The paint thinner liquids are primarily classified as medium petroleum distillate (MPD) in the Ignitable Liquids Database from the National Center for Forensic Science[43], and the paint thinner used in our study is also identified as MPD based on the ASTM criteria[22]. As evidenced in our GC/MS data and the literature, alkanes are the major chemical components in paint thinner products, sometimes blended with other aromatics or oxygenated solvents. However, the ionization of alkanes by DART-MS is challenging [37], and the ionization efficiency for producing protonated ions is considerably lower than that for alkyl ethers such as glycol ethers due to the lack of charge affinity functional groups in the structures. The selective sensitivity for the detection of less volatile glycol ethers could be a significant advantage of DART-MS for the analysis of paint thinner, which leads to more consistent and reproducible mass spectral profiles, reducing the impact of weathering degree and weathering temperature factors. On the other hand, the ion clusters in Region (b) changed among different samples, and especially for the 90-95% weathered samples, their relative intensities were much lower. In addition, these peaks in the 90-95% weathered samples prepared at 90 and 210 °C were further reduced in their intensities, indicating weathering temperature also played a role in the DART-MS spectral variation, and these compounds might evaporate faster than glycol ethers in the paint thinner under high temperatures.

The PCA score plot based on the DART-MS spectral data with the weathering degree factor labeled is shown in Figure 7. The first two principal components (PC) accounted for cumulative proportions of the variance in the data of 76.3%, corresponding to 55.1% and 21.2%, respectively, for PC1 and PC2. Compared with the PCA score plot with the GC/MS TIC profiles (Figure 2B), the paint thinner samples were not well clustered based on the weathering degree factor in Figure 7. The overlapping of the paint thinner sample objects in Figure 7 indicates the significant similarity of the DART-MS spectral profiles among the samples with different experimental treatments.

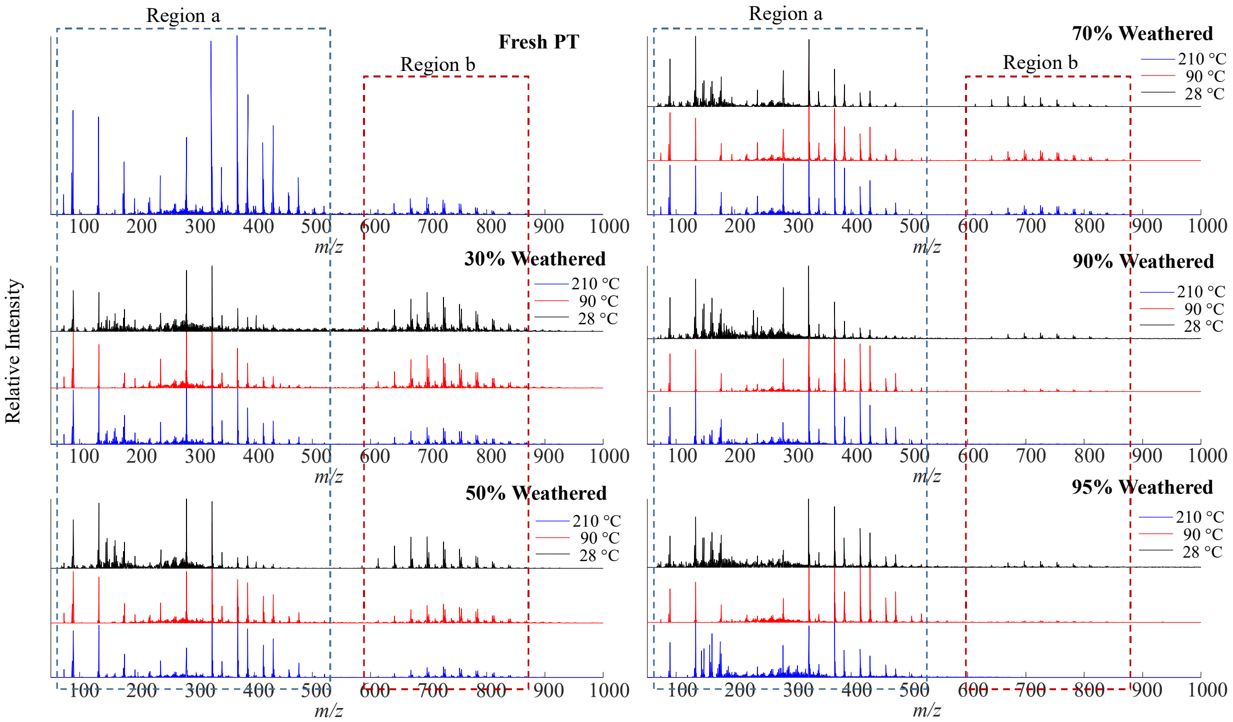

Figure 6. DART-MS spectra for fresh and weathered paint thinner samples. Samples were weathered at different temperatures (i.e., black spectra for room temperature, red spectra for 90 °C, and blue spectra for 210 °C). Each spectrum represents the average of the triplicate set of spectra.

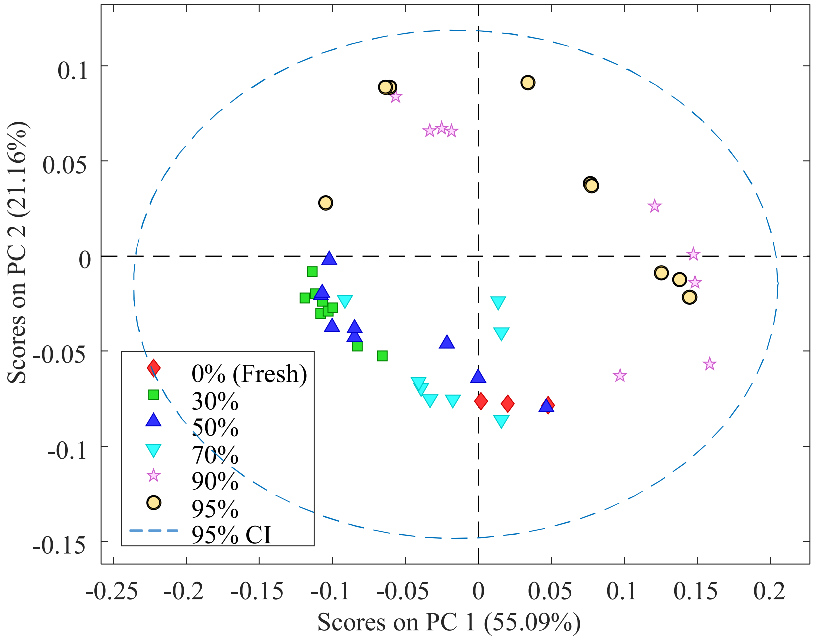

Figure 7. Principal component analysis score plots for paint thinner DART-MS spectral data. The percent variance spanned by the principal components is given in parentheses with the absolute variance. Data is mean-centered and normalized to the unit vector before performing PCA.

1.3.3 Quantitative Analysis of Variations in GC/MS and DART/MS Profiles by ANOVA-PCA

Although there are existing research studies on the impacts of weathering degree and temperature factors for GC/MS profiles of ILRs, a quantitative evaluation of both factors for IL profiles is limited. How these factors affect DART-MS profiles is largely unknown. Gasoline as a potential ignitable liquid used in an arson fire has been studied more extensively, but other common ILs, such as paint thinner, were not well understood. Another objective of this study was to statistically evaluate the effects of the weathering degree and temperature on the chemical profiles of paint thinners based on GC/MS and DART-MS analysis with chemometrics.

As described in the Experimental Section, each ignitable liquid was weathered to 5 different extents at three different temperatures and prepared in triplicate. Three major factors need to be considered to evaluate the chromatographic or spectral profile changes by GC/MS or DART-MS: weathering degree, weathering temperature, and replicate. Figure 8 shows an example of GC/MS data processing for weathered paint thinner samples by ANOVA-PCA. Total ion chromatograms (TIC) of weathered paint thinner samples (Figure 8A) follow the expected trend:

the relative quantities of less volatile compounds eluted at longer retention times are higher in the heavily weathered samples (e.g., 95% weathered paint thinner) because the more volatile compounds evaporate faster than, the less volatile compounds. However, the temperature factor was confounded with the weathering degree factor, and its effect was hardly perceptible. Therefore, the data matrix was decomposed into matrices corresponding to weathering degree and temperature factors, respectively (Figure 8B and 8C) by the ANOVA-PCA method so that the significance of each factor can be evaluated independently and quantitatively. Notably, the subset matrices for replicate factor and residuals were also calculated but not shown in Figure 8. To visualize the effects of the factors, PCA score plots (Figures 8D and 8E) were constructed using the respective factor matrices with the residual matrix, and the separation among different levels of each factor indicates the significant changes in TIC profiles affected by the factor. ANOVA-PCA differs from the other commonly used multivariate factor analysis methods, such as ANOVA-simultaneous component analysis (ASCA), in the way the factor matrices are analyzed. ASCA does not add the residual matrix to the effect matrices before PCA; therefore, the significance of the factor versus the residual error cannot be compared directly. Score plots obtained with ANOVA-PCA show the grouping of samples for the different levels of the independent variable. Table 2 shows the statistical analysis of the variance affected by the experimental factors in the GC/MS TIC profiles of paint thinners. The weathering degree factor contributed about 93.4% variance to the total variance, indicating this factor caused the most significant changes in the GC/MS TIC profiles, which agreed with the expectation and the discussion in Section 1.3.1. The temperature factor only led to a 2.1% total variance, but it was determined to be a considerably significant source of variations after comparing with the residue matrix with a *p*-value of 0.001. No significant difference was observed among the analytical replicates, which only accounted for less than 0.1% of the total variance. About 4.4% of the total variance could not be explained by the three experimental factors in the study, so the weathering degree and temperature factors captured most of the variations (>95%) of the paint thinner profiles by GC/MS TIC. Combined with PCA score plots (Figure 8) and ANOVA results (Table 2), the ANOVA-PCA method provided a qualitative and quantitative approach to analyze complex multivariate data matrices (i.e., paint thinner GC/MS TIC profiles). It can be expanded to investigate the chemical profile changes of various studies with multi-experimental factor design.

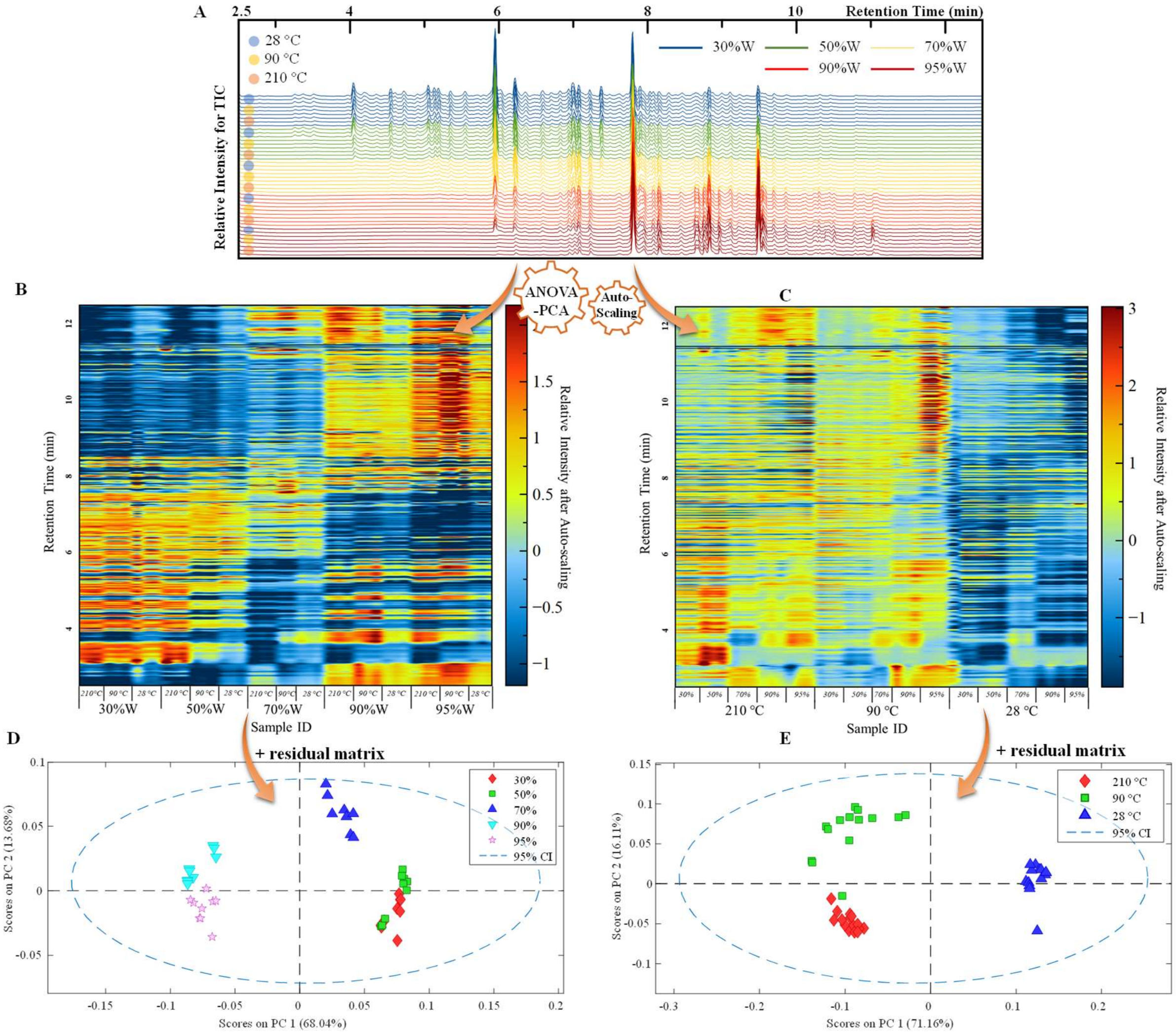

Figure 8. Total ion chromatogram (TIC) of GC-MS for the weathered paint thinner samples (A), the subset data matrices for the weathering degree factor (B) and weathering temperature factor (C) after ANOVA partition and auto-scaling data processing, and their respective PCA score plots (D and E). Note: samples were evaporated to 30, 50, 70, 90, and 95% by mass at 28, 90, and 210 °C.

Table 2. Analysis of Variance for the paint thinner GC/MS TIC and DART-MS spectral profiles

Data Type	Source of Variation	df	SS	Average SS	F value	*p*-value	F-Crit	Contribution to Total Variance
GC/MS TIC	Weathering degree	4	5.543	1.386	186.3	$<<10^{-3}$	2.6	93.4%
	Temperature	2	0.125	0.063	8.4	0.001	3.3	2.1%
	Replicate	2	0.007	0.004	0.5	0.624	3.3	0.1%
	Residuals	36	0.260	0.007				4.4%
DART-MS spectrum	Weathering degree	4	3.802	0.950	5.4	0.002	2.6	26.4%
	Temperature	2	3.531	1.766	10.0	0.0003	3.3	24.5%
	Replicate	2	0.696	0.348	2.0	0.154	3.3	4.8%
	Residuals	36	6.359	0.177				44.2%

ANOVA-PCA was also applied to process the DART-MS spectral matrices, and the statistical results are shown in Table 1. Although weathering degree and temperature factors still contributed significantly to the total variance of the data matrices, about 44.2% of the variability in the data (i.e., residuals) cannot be explained by these factors, which could be caused by the instrumental response variation and/or sample preparation variation. The ANOVA-PCA score plots for weathering degree and temperature factors based on the DART-MS data matrices are shown in Figure 9. In Figure 9A, the samples were not completely separated based on different weathering degrees, but the effect of weathering degrees on the DART-MS data can be observed from the shifts of group means with respect to the first principal component. For example, the heavily weathered samples (i.e., 90% and 95% weathered samples) were distributed in the data space with the negative scores of PC1, whereas most of the other samples were scattered with positive PC1 scores. Further examining the variable loadings (data not shown) in Figure 9A shows a significantly positive peak at *m/z* 80, corresponding to the positive clusters of paint thinner samples in Figure 9A. Though the compound contributing to this ion was not identified, this compound should be more volatile than the glycol ethers and more susceptible to the impact of experimental factors such as weathering degree because this signal became non-detectable in the heavily weathered samples (Figure 6). The samples representing the temperature factor have a mild separation between the 28 °C group and higher temperature groups (90 and 210 °C) based on the scores on PC1 in Figure 9B. The examination of the loading plots suggests the separation was contributed from the peak cluster in Region (b), and the results agree with our observations in Figure 6 and the previous discussion in Section 1.3.2. The samples prepared under 90 and 210 °C are spatially distributed without a clear grouping in Figure 9B, indicating that the residual matrix added significant noise to the submatrix for the temperature factor, which makes the observation of DART-MS spectral variations very challenging.

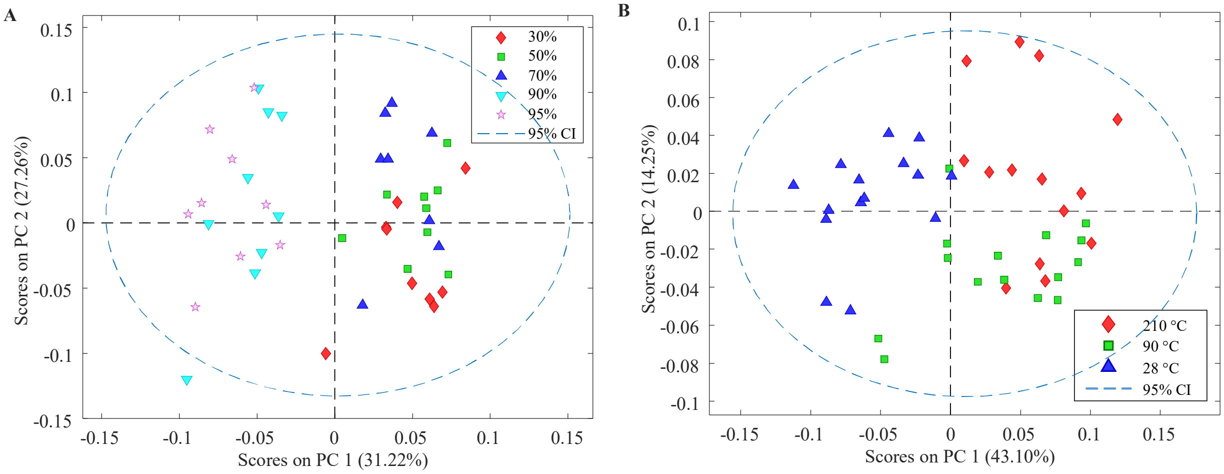

Figure 9. PCA score plots for weathering degree factor (A) and weathering temperature factor (B) based on the DART-MS spectral profiles after ANOVA partition.

1.3.4 Comparison of Different Paint Thinner Samples and Other ILs

Another set of paint thinners with various packages and brands was obtained to compare different paint thinner products. In addition, selected ILs, including torch fuel, lighter fluid, Japan Drier, and gasoline, were also prepared using the same procedures as the paint thinner samples: they were evaporated to different extents under three temperatures. All the samples were analyzed by both GC/MS and DART-MS. The PCA score plots are shown in Figure 10, and the GC/MS TIC profiles and DART-MS spectral profiles for different ILs are included in Figures 11-12. The paint thinner and Japan drier are both identified as medium petroleum distillate based on the ASTM E1618-19 criteria and the National Center For Forensic Science classification[22, 23], and have shown similar GC/MS TIC profiles in our study; therefore, they clustered close to each other in Figure 10C. However, their profiles are distinctive in the DART-MS spectra: the signature polymeric glycol ether ions were not observed in the Japan Drier mass spectra; therefore, the paint thinner and Japan Drier were well separated on the PCA score plot (Figure 10B).

On the other hand, the DART-MS spectra of the gasoline and torch fuel samples showed a distribution near the paint thinner samples (Figure 10B); however, their GC/MS TIC profiles differed from those of the paint thinner samples. So this shows that the GC/MS and DART-MS data can be used synergistically when reporting the positive identification of IL; that is, the GC/MS profiles can be used to classify the ILs into one of the ASTM categories, and additional positive detection of IL by DART-MS analysis can narrow down the list of specific IL products in the same category that are possibly associated with the fire. PLS-DA models were constructed by using GC/MS TIC and DART-MS spectral profiles of different ILs (excluding newly collected paint thinner samples) and evaluated with four Latin partitions and 100 bootstraps for the classification of ILs based on their types[24], and the classification rates are 99.97 ± 0.02% and 99.80 ± 0.08%, respectively. The result indicates that both data representations could be used to distinguish the ILs.

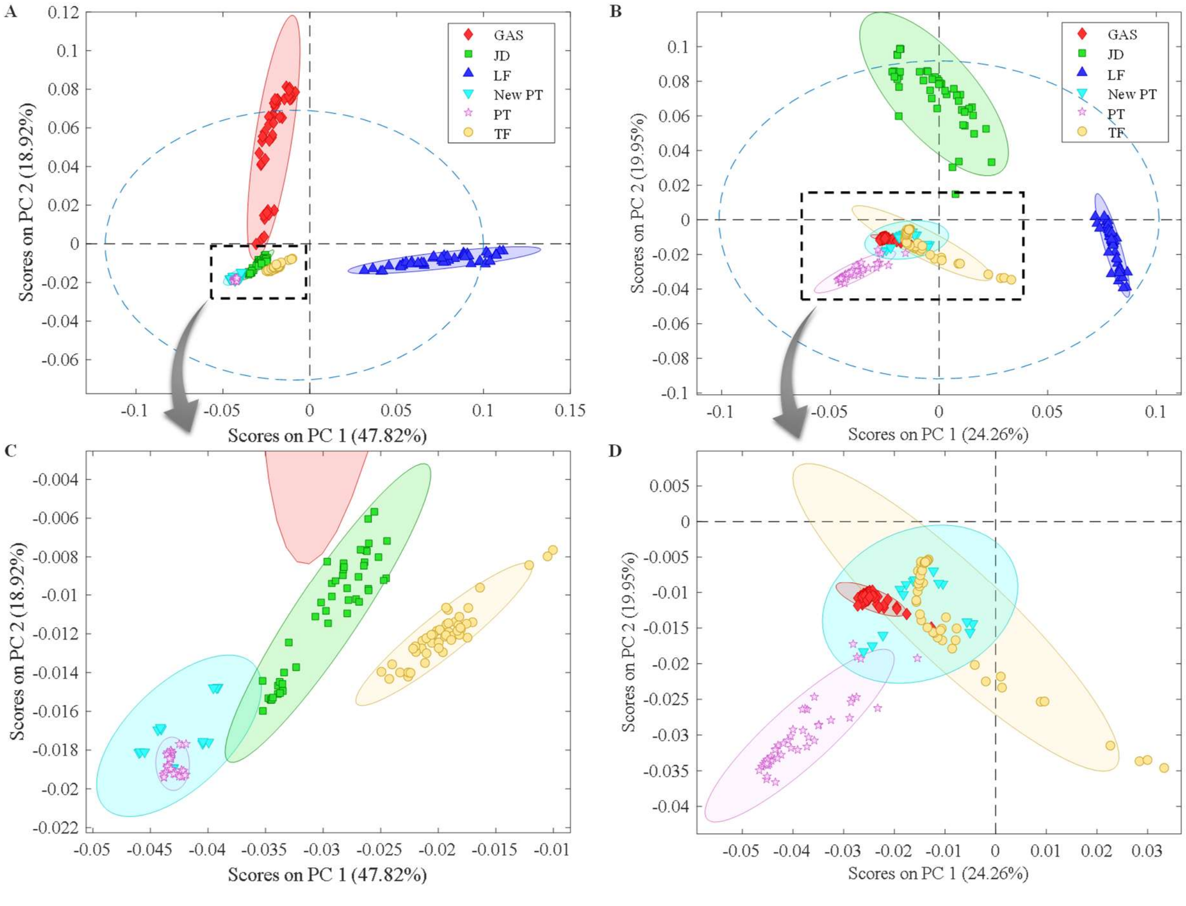

Figure 10. PCA score plots for different ILs based on the GC/MS TIC data (A) and based on the DART-MS spectral data (B). Selected regions are enlarged and shown in (C) and (D). GAS: Gasoline; JD: Japan drier; LF: Lighter fluid; PT: Paint thinner; TF: Torch fuel; New PT: newly collected paint thinners including KS plastic bottle PT, KS white metal bottle PT, KS blue metal

bottle PT, KS Barco PT, and Crown PT (Details available in Table S1). A 95% confidence interval is drawn around the mean of each class.

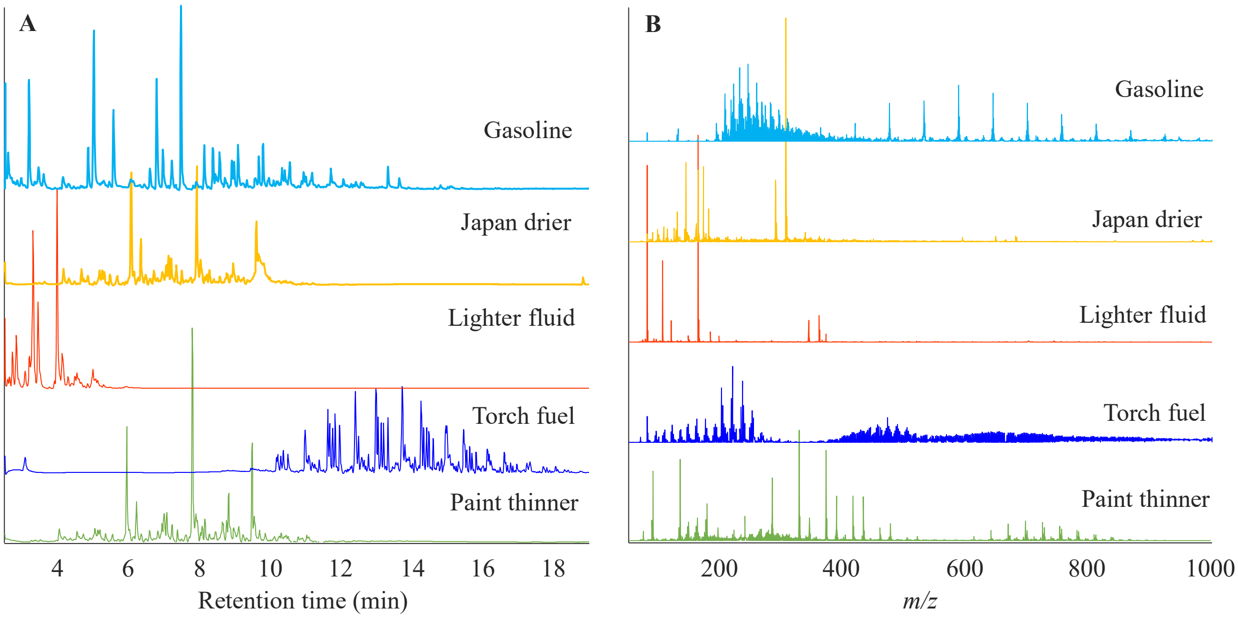

Figure 11. Average GC/MS TIC profiles (A) and average DART-MS spectral profiles (B) for different ILs (n = 45).

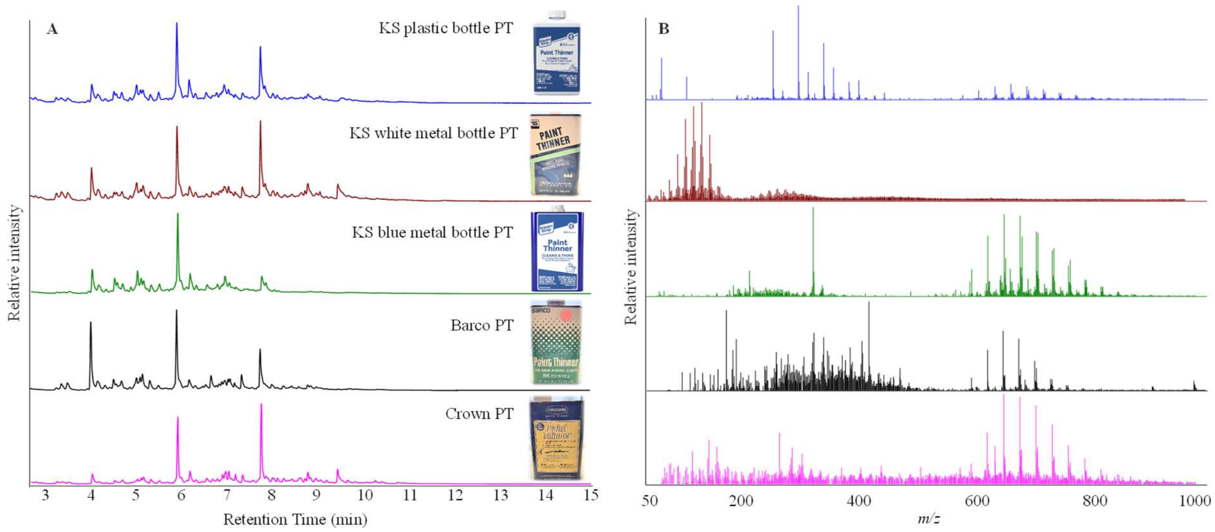

Figure 12. Representative GC/MS TIC profiles (A) and DART-MS spectral profiles (B) for different paint thinners.

Among paint thinner samples with different packages and brands, their GC/MS TIC profiles are very similar (Figure 12A). Most of the chromatographic peaks occur in the range of

C_8-C_{12} alkanes (medium petroleum distillates range). All seven compounds identified in Figure 3 were observed in other paint thinner products with slightly different relative intensities. This trend agreed with their distributions on the PCA plot (Figure 10C), in which scores for the new paint thinner collection (light blue triangle) overlapped with those for the paint thinner samples in the weathering study (purple stars). However, the DART-MS spectra among different paint thinner products showed distinctive profiles even for the same brand (i.e., KS plastic bottle PT *vs*. KS metal bottle PT in Figure 12B). The ion clusters for the high mass range in DART-MS spectra, e.g., *m/z* 550-1000 in Region (b) in Figure 3, were found for four of the five new paint thinner products, whereas the ions attributed to glycol ether derivatives were observed in only one of the paint thinners. This difference is also reflected in the PCA plot, where the two groups are split (Figure 10D). It is worth noting that the KS plastic bottle PT has the same package as the one used in the weathering study but was purchased 12 months after; therefore, both GC/MS TIC and DART-MS spectral profiles of this product closely matched with data collected in the weathering section. The main application of the GC/MS-based standard method (i.e., ASTM E1618-19) is to identify ILs as belonging to one of the seven major classes or the miscellaneous class primarily based on the compound profiles for alkane, cycloalkane, aromatic, polynuclear aromatic, and oxygenates[22]. As demonstrated in Figure 10A, the GC/MS method has shown superior resolving power to distinguish different types of ILs. In contrast, the DART-MS method cannot offer sufficient spectral information to classify the ILs into the ASTM classes because of its insensitivity to alkanes and aromatics. But DART-MS spectral profiles could aid in the further characterization of IL by providing brand- or liquid-specific data for different groups of chemicals, such as ion clusters for glycol ether derivatives, and this information should be considered as orthogonal to the GC/MS data. It could be especially valuable when the substrates or combustion of materials at the fire scene interfere with the GC/MS profiles of ILs. Future work will examine the matrix effects of the substrate materials on the analysis of ILs by both GC/MS and DART-MS. In summary, both GC/MS TIC and DART-MS data produce discriminative data profiles for IL classification, and DART-MS can complement the existing GC/MS method for identifying ILs.

1.4 Conclusions

In this section, paint thinner samples were weathered at different conditions and then analyzed by GC/MS and DART-MS. While the GC/MS TIC profiles have shown significant variations affected by the weathering degree and temperature, the DART-MS spectral profiles, indicating a unique ion pattern for glycol ether derivatives, are more resistant to the weathering process. ANOVA-PCA has been applied to study the variations of both GC/MS TIC and DART-MS spectral profiles caused by the weathering degree and temperature factors, and the contribution to the total variance from each factor was evaluated qualitatively and quantitatively. The identification of less volatile compounds, such as glycol ether derivatives, from DART-MS analysis, could be valuable for the detection of ILR because they were more likely to be retained after weathering or even burns. Though we have demonstrated that DART-MS analysis provides discriminative information for distinguishing IL samples, it does not replace the GC/MS method but rather enhances or supplements the existing GC/MS approach for identifying IL.

Section 2. Investigation of the Weathering Effect on the Chemical Profile of Less Volatile Components in Other Ignitable Liquids

2.1 Introduction

In the United States, fires are responsible for the loss of billions of dollars annually, and 13% of all fires in the United States are due to arson.[25] Furthermore, approximately 500 people die each year in the U.S. due to arson fires. Despite this fact, arson investigations result in an astonishingly low arrest rate of roughly 19 % and an even lower conviction rate of about 2%.[3] The inherent difficulty of the chemical analysis of fire debris for ignitable liquids is a significant contributing factor. In the event of a property fire or even an explosion, the remains provide evidence for arson investigators. The most common accelerants used in arson are gasoline, kerosene, lighter fluid, paint thinners, and solvents.[3]

Ignitable liquids, especially in weathered liquid samples, have been the subject of many studies for arson investigation purposes. To compare residues in fire debris with ignitable liquid sample references, the ignitable liquid sample references are usually weathered to a certain extent. These are then used to compare the peak abundances of chromatograms. Some researchers concluded that casework samples frequently provided adequate quality matches when the comparison ignitable liquids were weathered between 50% and 75%.[26] On the other hand, the highly elevated temperatures of structural fires should cause more weathering than 50–75%, especially for more volatile ignitable liquids such as gasoline. One possible explanation for this phenomenon is entrapment, which assumes that "*a certain portion of the pristine liquid is trapped* *in the pores of the substrate, and these relatively non-weathered residues are then extracted during the equilibrium conditions of headspace extraction*."[19]

The weathering of the ILs ranging from 90 – 210°C was implemented in this section to make the weathering more comparable to the actual casework of arson. DART-MS was used to analyze ignitable liquids due to its high sensitivity to less volatile compounds. The knowledge of the chemical profiles of different ignitable liquids under various weathering conditions can assist in solving not only arson cases but also in the remediation of fuel spills in the environment and understanding properties related to ignitable liquids in petroleum products in general.

2.2 Methods

2.2.1 Weathering of ILs

For this section, four common products containing ignitable liquids (ILs) were included: gasoline, Zippo Lighter Fluid, torch fuel, and charcoal fuel. Aliquots of varying amounts were weathered at room temperature, 90 °C and 210 °C – to five different percentages: 30, 50, 70, 90, and 95 %. Glass vials and amber containers were used for the weathering process of the samples in room temperature and elevated temperatures, and an aluminum block on a hot plate was used to heat the samples to the elevated temperatures.

The weathering percentages were verified by calculating an expected value for the specific weathering percentage beforehand.

$$M_{IL} = (M_0 + M_{IL}) - M_0 \dots\dots\dots (1)$$

This equation was used to calculate the weight of the IL (M_{IL}), where M_0 is the weight of the container with the lid.

$$M_{IL} \ = (100\% - desired\ percentage\ of\ weathering) \times M_{IL} \dots\dots\dots (2)$$

This equation (2) was used to calculate the expected weight of the ignitable liquid after the desired percentage of weathering (M_{IL2}). Setting fixed percentages and weathering temperatures enables observation of the effects that varying temperatures and weathering degrees have on the ILs and the overall weathering process.

After weighing the containers, different aliquots of each IL were placed in the containers. For 30% and 50% of weathering, 2 mL of the ILs were added to containers, 5 mL for 70%, and a higher amount of 16 mL for 90% and 95% of weathering. This was done to minimize the IL used but also to make sure that there was enough sample for both GC/MS and DART-MS analysis after the sample preparations, especially for the higher weathering percentages. The ILs were transferred to tared containers and weighed to calculate how much they would need to be weathered to reach the desired weathering percentages. Only two ignitable liquids were weathered at a time to prevent cross-contamination. The empty containers of all the samples were weighed. The amber containers with the bigger opening were used for the samples weathered at room temperature and for the higher percentages at the elevated temperatures since they contained more liquid; smaller vials were used that would fit in the aluminum block for the samples that were weathered at lower percentages for 90 and 210 °C. The samples that were weathered at room temperature were left inside a fume hood until the desired weathering percentage was reached. For weathering at 90 and 210 °C, an aluminum block was placed on a hot plate and was adjusted to the right temperature using a thermometer before weathering. After each weathering, the glass vials and amber containers were capped and stored in the refrigerator to minimize additional weathering.

Charcoal fuel was also analyzed through GC/MS and DART-MS, but due to its difficulty in weathering at room temperature and 90 °C, only data from samples weathered at 210 °C (30-90%) were obtained.

2.2.2 Sample Preparation for GC-MS and DART-MS

The instruments for this experiment were GC/MS and DART-MS with the QuickStrip™ module for analysis of the samples. The QuickStrip™ Sample Cards were used to spot samples and blanks in each of the twelve slots and conduct analysis using the DART-MS.

For the GC/MS samples, each GC vial contained 20 µL of the desired sample, 20 µL of the internal standard (1-bromohexadecane, 10 mg/mL), and 1mL of chloroform as the solvent. Each sample was prepared in triplicate. For the DART samples for the gasoline and torch fuel, each DART vial contained 50 µL of the desired sample and 950 µL of chloroform, which was a 20 × dilution. The charcoal fuel samples were diluted at a higher rate compared to the paint thinner and torch fuel to prevent carryover signals in the subsequent runs. Similarly, charcoal fuel and lighter fluid were diluted at an even higher rate. Each DART sample of charcoal fuel had 20 µL of the IL sample and 980 µL chloroform (50 × dilutions). For lighter fluid, each sample had 5 µL of the IL sample and 995 µL chloroform (200 × dilutions). Each sample for DART was also prepared in triplicate. For both GC-MS and DART-MS, fresh samples of all four ILs were also prepared in triplicates as the control set. A total of 162 samples were analyzed for each GC/MS and DART-MS.

2.2.3 Instrument Parameters

GC/MS has been developed in the lab by following the ASTM E1618 method. GC/MS analyses were performed on a Shimadzu QP2010S with an autosampler. The analytes were separated on a ZB-35HT capillary column of 30 m × 0.25 mm × 0.25 µm with the stationary phase of 35% diphenyl/65% dimethylpolysiloxane (Phenomenex, Torrance, CA) using the following oven temperature program at a constant flow of 1 mL/min: 50 °C, hold for 1 min, ramp at 20 °C/min to 280 °C, hold for 10 min. The transfer line and ion source temperatures were both maintained at 280 °C. The full scan mode was selected for the mass spectrometer with the scan range from *m/z* 30 to 350**.**

The DART-MS method from a previous publication (Barnett et al., 2019) was adopted. A DART ion source (IonSense, Inc., Saugus, MA) is coupled to a Thermo LTQ XL mass spectrometer (Thermo Scientific, San Jose, CA). The QuickStrip™ module was used with the QuickStrip™ Sample Cards (IonSense, Inc., Saugus, MA). The ionization gas is helium for all the DART-MS experiments. The DART gas heater was set to 350 ºC, and the mass spectra were collected in an *m/z* range of 50-1000 in positive-ion mode. In order to prevent possible carryovers in the subsequent runs of the lighter fluid, the gas heater was set to 500 ºC for lighter fluid samples.

2.2.4 Analysis of ILs

All the samples for the GC/MS analysis were run in one sequence. For DART-MS, the samples in triplicates were spotted in each of the twelve slots of the QuickStrip™ Sample Card, with blanks in between each set of triplicates for background subtraction. In between runs, the QuickStrip™ module was cleaned using methanol to reduce the carryover signals from the previous run to the next run. As the samples were analyzed by GC/MS and DART-MS, the chromatographic data was collected and analyzed using the Shimadzu GC/MS Solutions and the Thermo Xcalibur data analysis software. The data (average mass spectrum) for each sample for DART-MS was exported to Excel after background spectrum subtraction.

2.3 Results

2.3.1 GC/MS Results

A distinctive pattern corresponding to the extent of weathering was observed with the TIC of GC/MS for the gasoline shown in Figure 13. The GC/MS TIC profiles reflect the expected trend: the volatile compounds become undetectable for heavily weathered samples, whereas the chromatographic peaks for the less volatile and stable compounds dominate the TIC profiles. The ANOVA-PCA was used to study the impact of experimental factors such as weathering temperature and weathering percentages during the sample preparation process. Figure 14 shows the PCA plots for the gasoline on GC/MS for the two significant experimental factors: weathering extent and temperature. As shown in the score plots, the gasoline samples with a similar extent of weathering were clustered together. On the right-hand side of Figure 14 is the loading plot, showing the peaks affected by the weathering extent and weathering temperature factors. The ANOVA-PCA results indicate the weathering percentage was the major factor for the variance of the TIC data. For example, the variance contributions by weathering percentages and the weathering temperatures in the gasoline samples were 79% and 9.7%, as shown in Table 3. The replicate variance for the GC/MS data represents only 0.1% of the total variance, which indicates good reproducibility of the analysis.

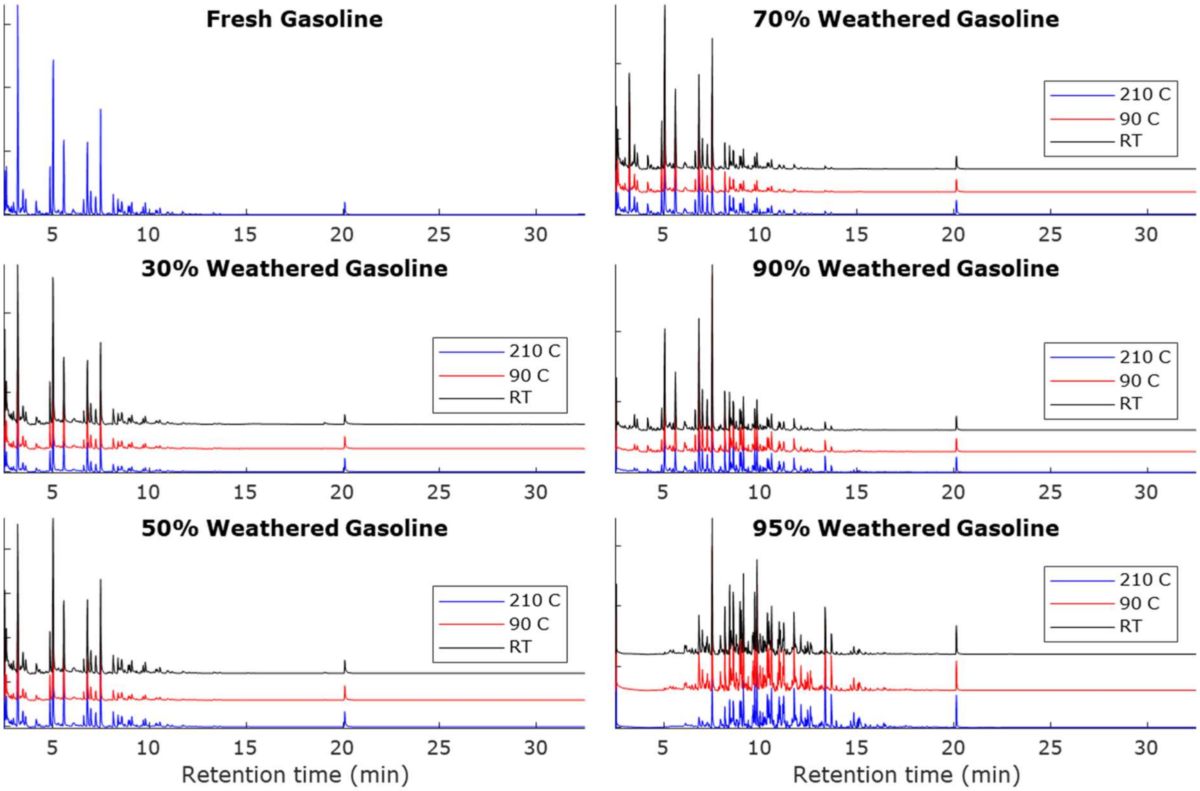

Figure 13. Fresh and weathered gasoline profiles by GC/MS

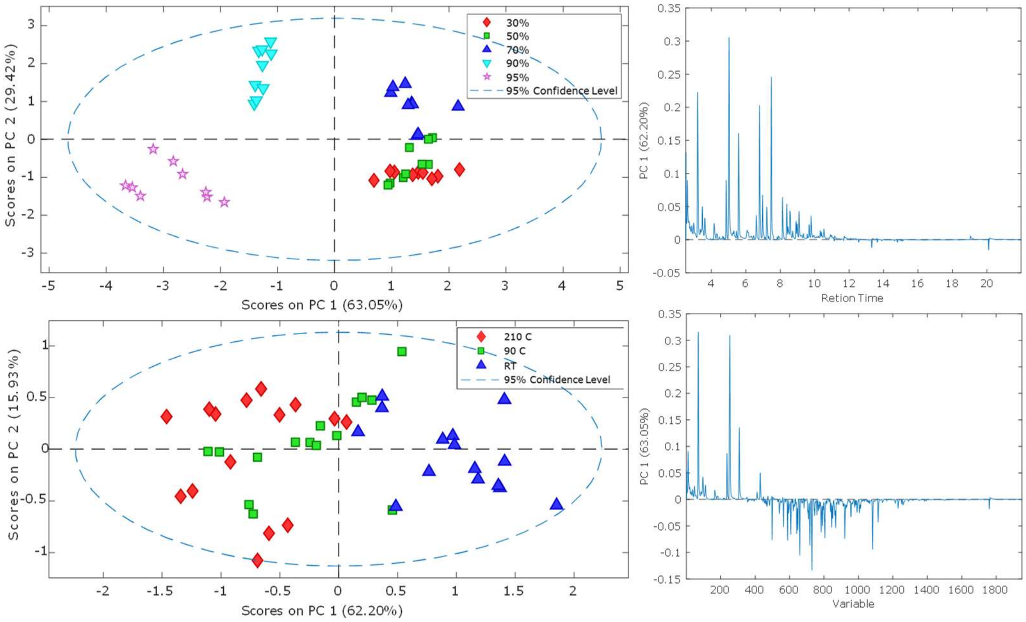

Figure 14. ANOVA-PCA of weathering degree factor (top) and temperature factor (bottom) based on GC/MS data of weathered gasoline samples. Score plots on the left and loading plots on the right.

Table 3. Analysis of variance for GC/MS data of the gasoline samples

	Source of variation	**n**	**SS**	**% of** the **total variance**	***p*-value**
gasoline samples	Grand Mean	45	257.3	100.0	
	Residuals	45	28.9	11.2	
	Weathering degree	5	203.1	79.0	9E-16
	Temperature	3	25.0	9.7	1E-05
	Replicate	3	0.3	0.1	8E-01

Similarly, the peaks eluted at early retention times in torch fuel and lighter fluid decreased and became lower as the weathering degree increased (Figures 15-16), indicating the loss of the more volatile compounds as the samples were further weathered. For torch fuel, the major peaks in the TIC appeared mainly in the retention time range of 8-15 min in the fresh samples, but more peaks were observed in the 12-18 min range for the TIC of 95% weathered samples, showing that the high molar mass and the less volatile components remained, and the more volatile compounds evaporated. For lighter fluid, the TIC profiles looked very similar throughout all the weathering degrees other than the relative lower intensities of the first several peaks in the TIC of heavily weathered samples.

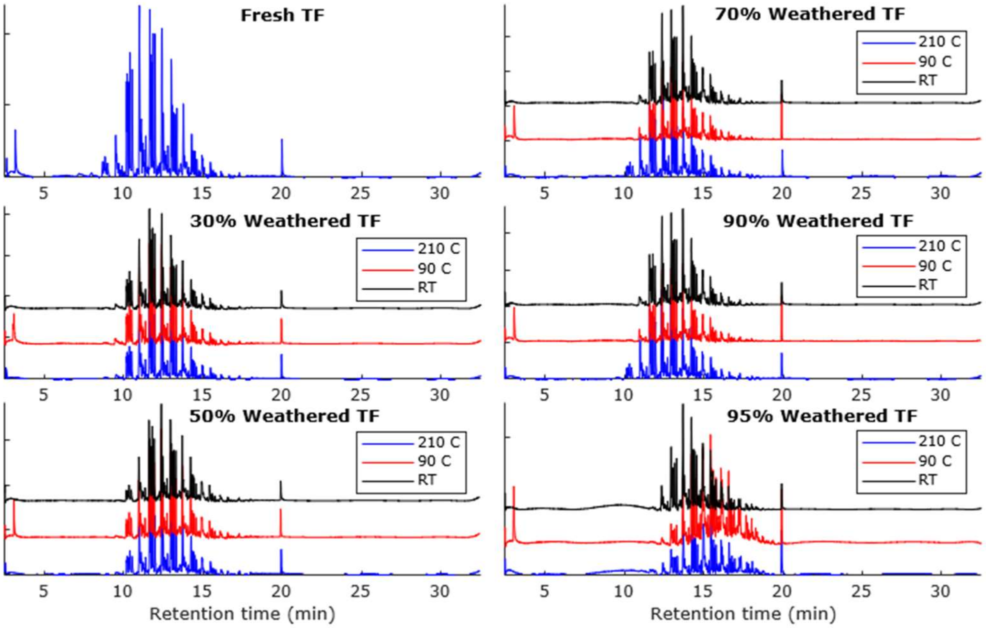

Figure 15. Total ion chromatograms (TIC) of GC/MS analysis showing compositional variations of torch fuel samples affected by weathering degrees and temperature factors.

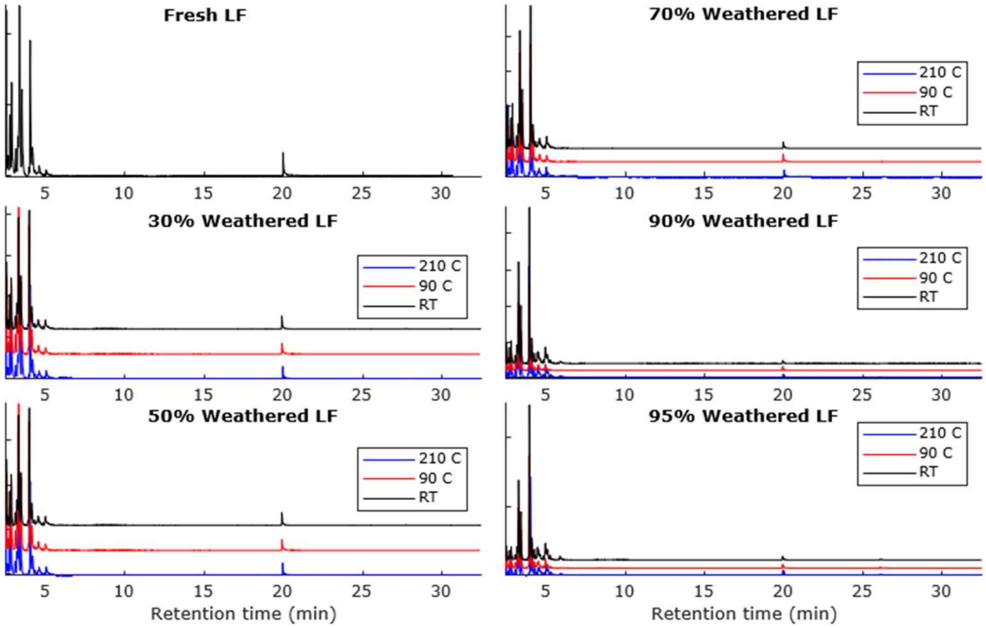

Figure 16. TIC of GC/MS analysis showing compositional variations of lighter fluid samples affected by weathering degrees and temperature factors.

ANOVA-PCA was used to obtain the score and loading plots of the results. ANOVA stands for "analysis of variance" and is used to partition the original matrix into subsets corresponding to the experimental factors. PCA stands for "principal component analysis" and is a visualization tool that shows the clustering of samples in the score plot. The loading plot, on the other hand, shows what features contribute to the clustering of the samples, where the positive peaks are more abundant in the samples in the positive coordinate of the score plot, and the negative peaks are more abundant in the samples in the negative coordinate. ANOVA-PCA also calculates the percentage of total variance contributed by the experimental factor.

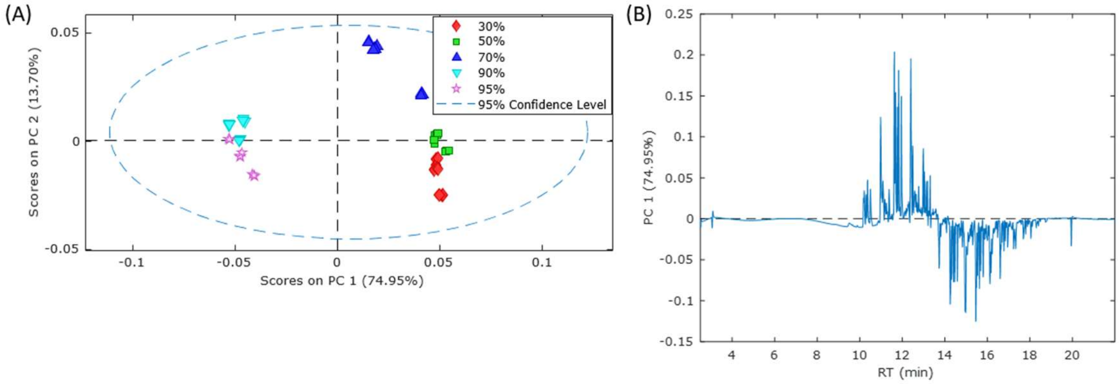

Figure 17. Score plot (A) and loading plot (B) from ANOVA-PCA of weathering degree factor based on the GC/MS TIC data of torch fuel.

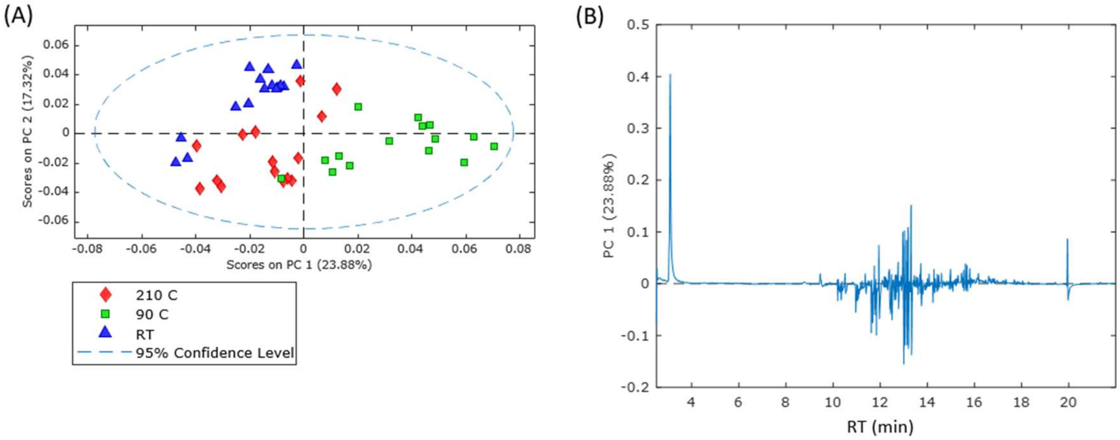

Figure 18. Score plot (A) and loading plot (B) from ANOVA-PCA of temperature factor based on the GC/MS TIC data of torch fuel.

The principal component (PCA) score plots obtained from the matrices correspond to the two factors, weathering degree and temperature. Comparing the two PCA score plots of torch fuel in Figure 17A and 18A, the score plot of the temperature factor does not show a clean separation between samples weathered at different temperatures. On the contrary, there are clear clusters between the weathering degrees, where the lower weathering degrees are clustered on the positive coordinate. The higher weathering degrees are clustered on the negative coordinate of the score plot (Figure 17A). Figures 17B and 18B show the variable loading corresponding to the score plots (Figures 17A and 18A, respectively). In the weathering degree score plot (Figure 17A), the PCA separated the weathering degrees in the positive clusters (30-70%) and negative clusters (90-95%). The PCA loading plot describes the characteristic ions that are positive in 30-70% and the characteristic ions that are negative in 90-95%. The same trends are observed in the temperature factor PCA score plot and loading plot, although no clear clusters can be seen in the temperature score plot. The same experimental factors evaluated by ANOVA-PCA in the PCA scores are described by pooled ANOVA in Table 4 below. The weathering factor contributed 83.4% variance to the data matrix and only 5.5% for the temperature factor. The replicate factor only counted for 0.2% variance, and the residual factor, variables that were not accounted for in the experiment, contributed 10.9% of the total variance. As a general rule, experimental factors with p-values less than 0.05 are regarded as statistically important, and with a p-value of 2.22×10^{-16} for the weathering degree factor and 0.00065 for the temperature factor, the weathering degree and temperature are important factors that significantly affect the torch fuel GC-MS TIC profiles.

Table 4. Analysis of variance for full GC/MS spectra data of torch fuel.

Source of Variation	n	df	SS	% of Total Variance	Average SS	F value	*p*-value	F-Crit
Grand Mean	45		11.16	100				
Residuals	45	36	1.21	10.9	0.033			
Weathered degree	5	4	9.31	83.4	2.32	68.8	2.22E-16	2.63
Temperature	3	2	0.61	5.5	0.306	9.059	0.00065	3.25
Replicate	3	2	0.022	0.2	0.011	0.337	0.71599	3.25

The PCA score plots in Figures 19A and 20A for the two factors in lighter fluid indicate the clustering of groups. The PCA score plot of the weathering degree factor shows separation where the lower weathering degrees (30-70%) have negative scores, and the higher weathering degrees (90-95%) have positive scores (Figure 19A). The varying temperatures in the PCA score plot for the temperature factor show a pattern of separation, with room temperature and 90 ºC having positive scores and 210 ºC having negative scores (Figure 20A). This separation between positive and negative is also shown in the PCA loading plots (Figures 19B and 20B). In the case of lighter fluid, both weathering degree and temperature factors are important in the analysis by GC/MS TIC profiles, having 63.1% and 28.4% of the total variance, respectively (Table 5).

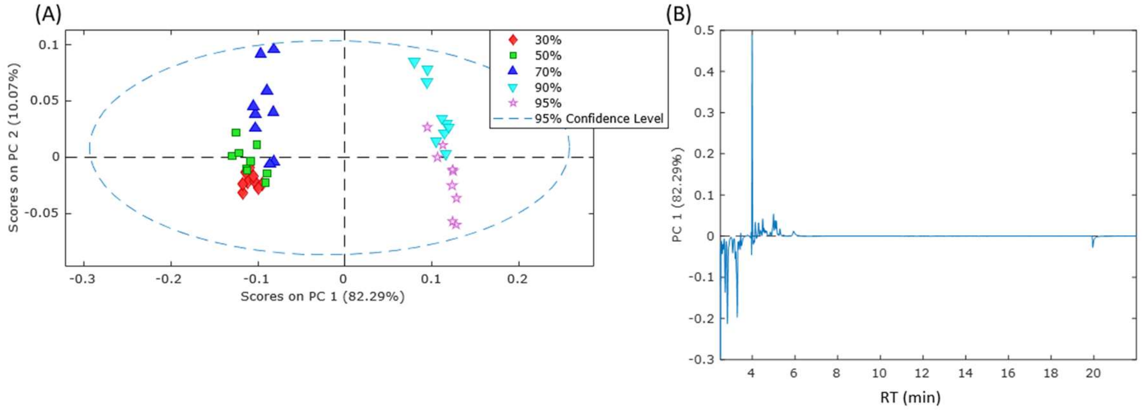

Figure 19. Score plot (A) and loading plot (B) from ANOVA-PCA of weathering degree factor based on the GC/MS TIC data of lighter fluid.

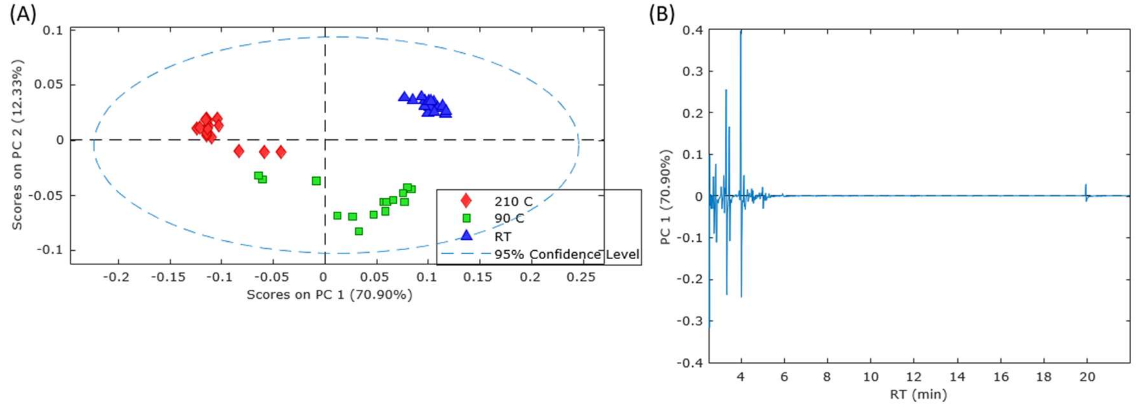

Figure 20. Score plot (A) and loading plot (B) from ANOVA-PCA of temperature factor based on the GC/MS TIC data of lighter fluid.

Table 5. Analysis of variance for full GC-MS spectra data of lighter fluid.

Source of Variation	n	df	SS	% of Total Variance	Average SS	F value	*p*-value	F-Crit
Grand Mean	45		2.81	100				
Residuals	45	36	0.23	8.2	0.0064			
Weathered degree	5	4	1.77	63.1	0.444	69.1	2.2E-16	2.63
Temperature	3	2	0.79	28.4	0.399	62.2	2.0E-12	3.26
Replicate	3	2	0.0069	0.2	0.0034	0.540	0.587	3.26

In Figure 21, the peaks at 19 min retention time that were present for 30-70% weathering are not present at 90%. In addition, more peaks are present at the 20-32 min retention time range in 90% compared to the lower weathering degrees. In Figure 22A, the PCA score shows a separation of 90% weathering from the other data, where it is clustered on the positive side of the PCA score plot with its characteristic ions on the positive side of the PCA loading plot (Figure 22B).

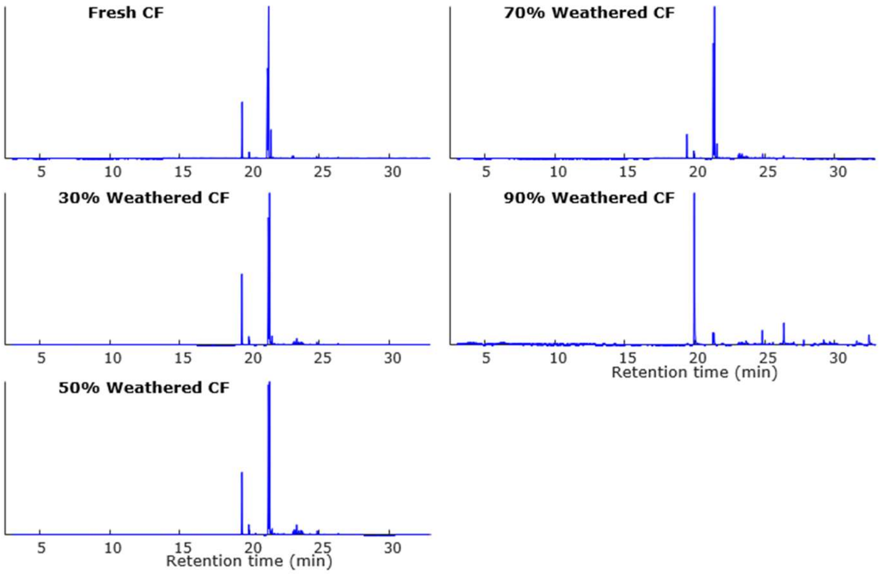

Figure 21. TIC of GC/MS analysis showing compositional variations of charcoal fuel samples affected by the weathering degree factor.

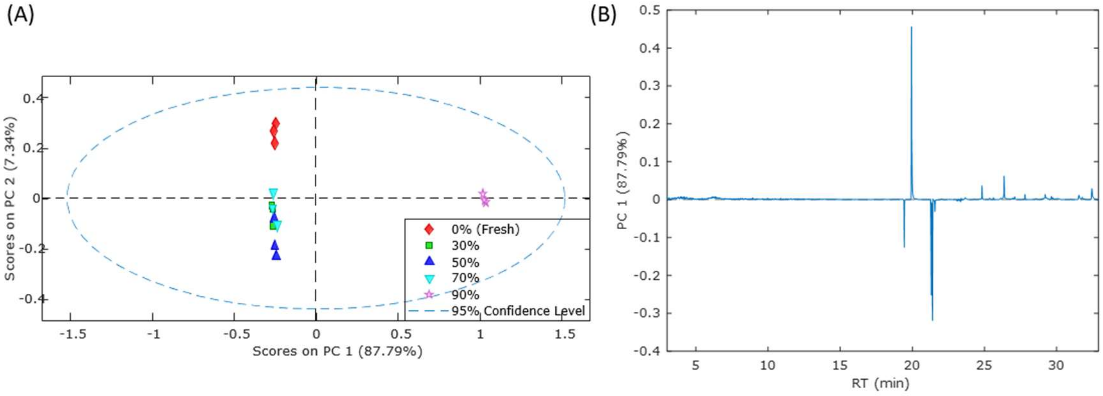

Figure 2. Score plot (A) and loading plot (B) from ANOVA-PCA of weathering degree factor based on the GC/MS TIC data of charcoal fuel.

2.3.2 DART-MS Results

In general, the DART-MS spectral profiles for gasoline samples were similar among different extents of weathering samples (Figure 23). As the weathering extent increased, only the less volatile compounds remained, and more volatile compounds were lost during the process. However, the characteristic ions in the DART-MS spectrum are contributed from the less volatile compounds (i.e., fuel additives), and the profiles are resistant to the weathering effect, as shown in Figure 23. To better understand the experimental factors, such as weathering degree and weathering temperature, ANOVA-PCA was applied to process the data collected. The results are shown in Table 6. The weathering degree was found to significantly impact the variations of DART-MS spectral profiles, although the fuel additive ions were relatively consistent among different weathered samples.

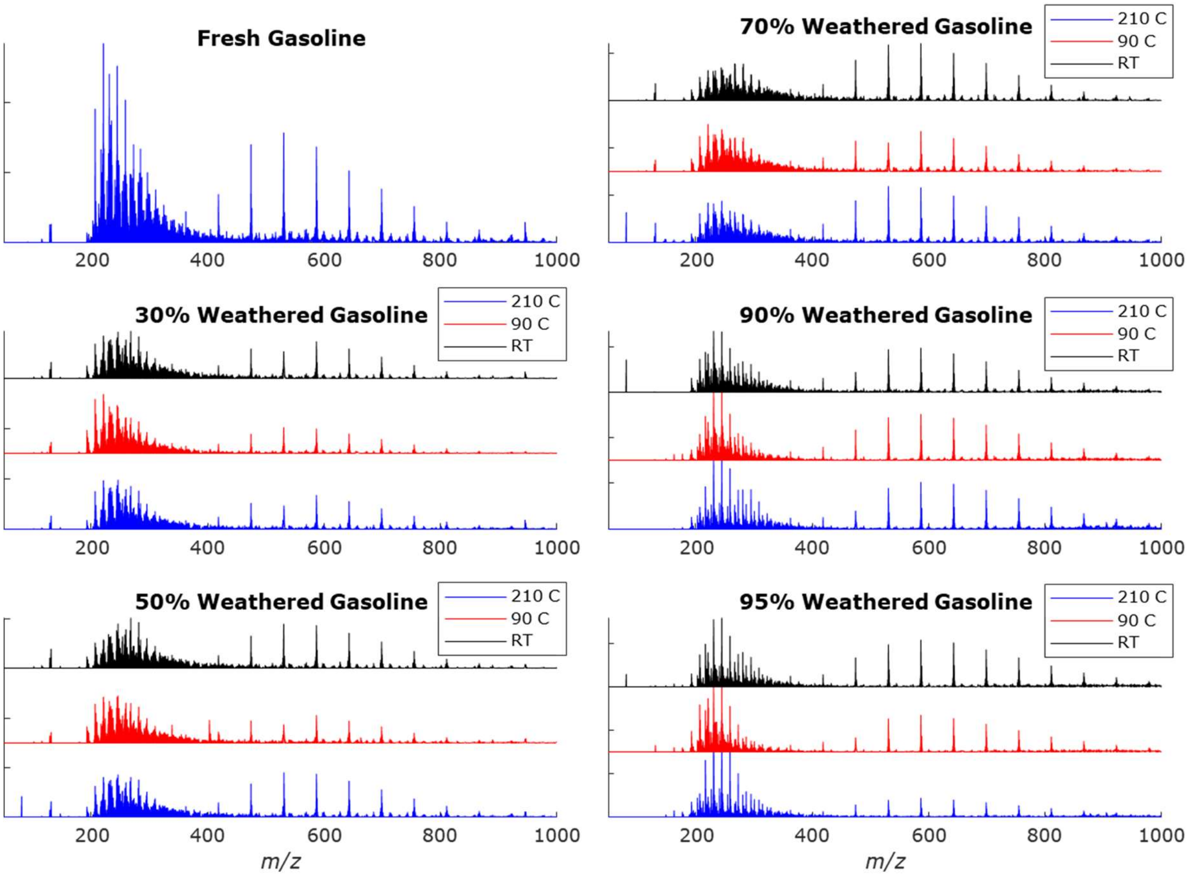

Figure 23. Fresh and weathered gasoline profiles by DART-MS

Table 6. Analysis of variance for DART-MS data of the gasoline samples

	Source of variation	**n**	**SS**	**% of total variance**	**p value**
gasoline samples	Grand Mean	45	5.9	100.0	
	Residuals	45	1.8	29.5	
	Weathering degree	5	3.5	58.8	4E-08
	Temperature	3	0.6	10.4	4E-03
	Replicate	3	0.1	1.3	5E-01

The DART-MS spectral profiles for the other two ILs appear in Figures 24-25. The relative peak profiles stayed similar throughout the weathering degrees. However, the two ILs showed different signals at varying temperatures. For torch fuel, there is a prominent difference in the peaks at 210 °C as compared to those at lower temperatures. The peaks in the *m/z* 100-300 range were not present in the samples weathered under 210 °C, indicating that the more volatile compounds have evaporated, and the high molar mass and the less volatile compounds are left. The major peaks in the lighter fluid profiles looked similar at 30-95% weathering.

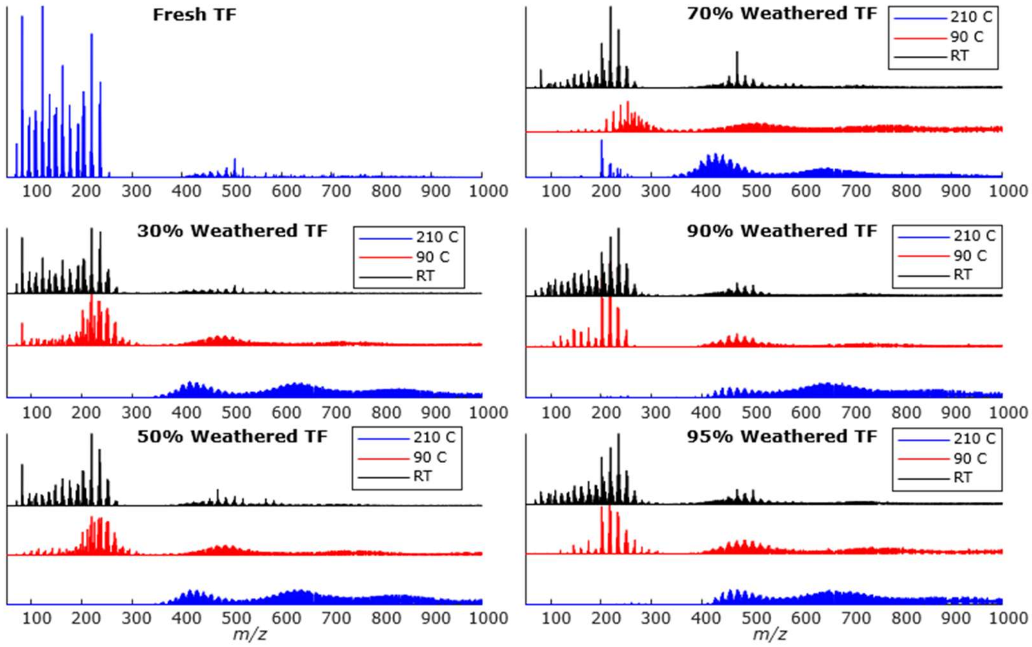

Figure 24. DART-MS spectral variations of torch fuel samples affected by weathering degrees and temperature factors.

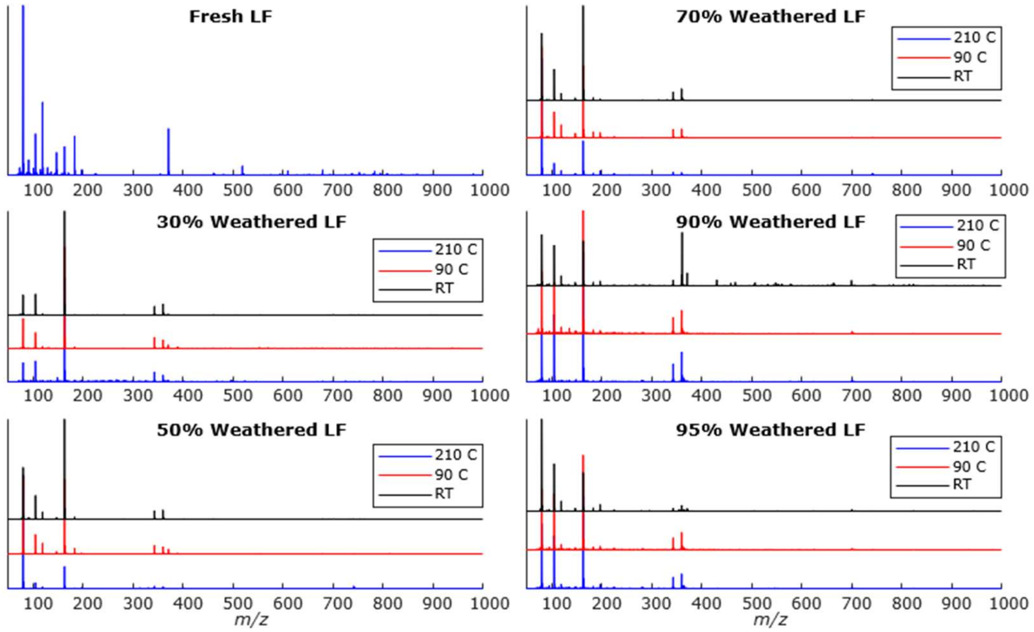

Figure 25. DART-MS spectral variations of lighter fluid samples affected by weathering degrees and temperature factors.

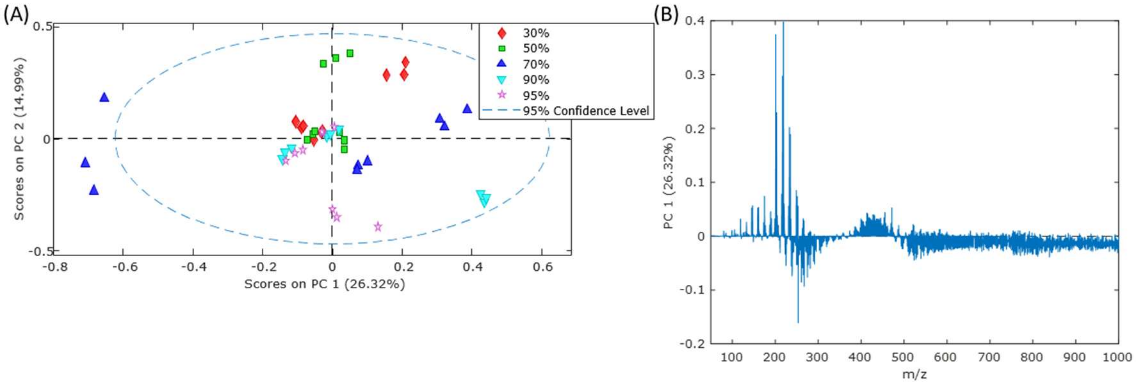

Figure 26. Score plot (A) and loading plot (B) from ANOVA-PCA of weathering degree factor based on the DART-MS spectral data of torch fuel.

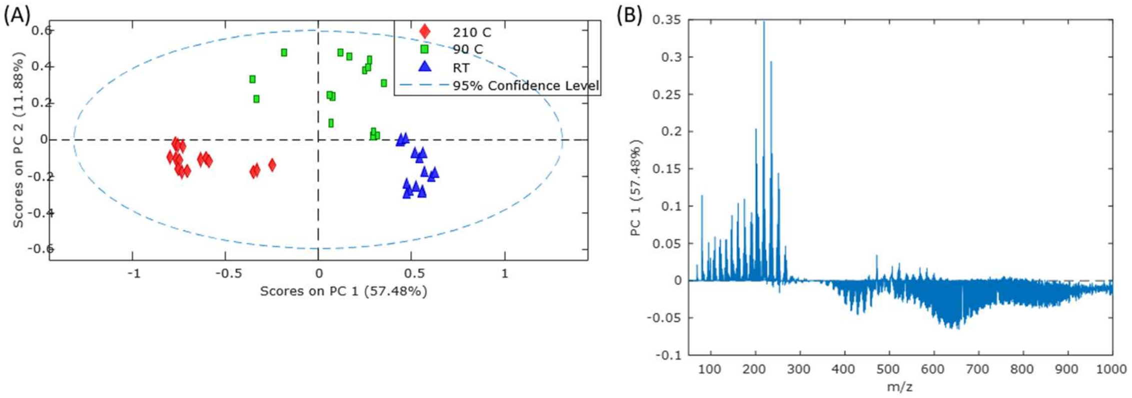

Figure 27. Score plot (A) and loading plot (B) from ANOVA-PCA of temperature factor based on the DART-MS spectral data of torch fuel.

For DART-MS, the score plots, loading plots, and the percentages of total variance were also obtained from ANOVA-PCA. From the two PCA score plots of torch fuel for both factors, the weathering degree factor does not show a clustering pattern (Figure 26A), while there is a clear separation between the samples weathered at different temperatures (Figure 27A). Figures 26B and 27B show the variable loading corresponding to the score plots (Figures 26A and 27A, respectively). In the temperature score plot (Figure 27A), the PCA separated the temperatures into the exclusively positive clusters (RT), the exclusively negative cluster (210 °C), and the predominantly positive clusters (90 °C). The PCA loading plot describes the characteristic ions that are positive at room temperature and 90 °C and those that are negative at 210 °C. The weathering degree PCA score plot and loading plot are arranged the same way, though, as shown in the score plot, no separation can be seen. The same experimental factors evaluated by ANOVA-

PCA in the PCA scores are described by pooled ANOVA in Table 7 below. The weathering factor contributed only 9.8% variance to the data matrix and 55.3% for the temperature factor. The replicate factor only accounted for 0.8% variance and the residual error contributed 34.1% variance. With a *p*-value of 0.0528 for the weathering degree factor and 2.9×10^{-8} for the temperature factor, the temperature is the most significant factor for the torch fuel DART-MS spectral profile.

Table 7. Analysis of variance for full DART-MS spectra data of torch fuel.

Source of Variation	n	df	SS	% of Total Variance	Average SS	F value	p-value	F-Crit
Grand Mean	45		22.47	100				
Residuals	45	36	7.66	34.1	0.212			
Weathered degree	5	4	2.20	9.8	0.551	2.59	0.0528	2.63
Temperature	3	2	12.42	55.3	6.21	29.18	2.9E-08	3.25
Replicate	3	2	0.174	0.8	0.0872	0.409	0.666	3.25

For lighter fluid in Figures 28A and 29A, the PCA score plots for weathering degree and temperature factors do not show clustering of groups. However, the analysis of the variance summary table shows that the total variance of the weathering degree factor is 34.5% with a *p*-value of 0.000123, and the total variance of the temperature factor is 3.8% with a *p*-value of 0.302. This indicates that the weathering degree factor can significantly affect lighter fluid DART-MS spectral profiles.

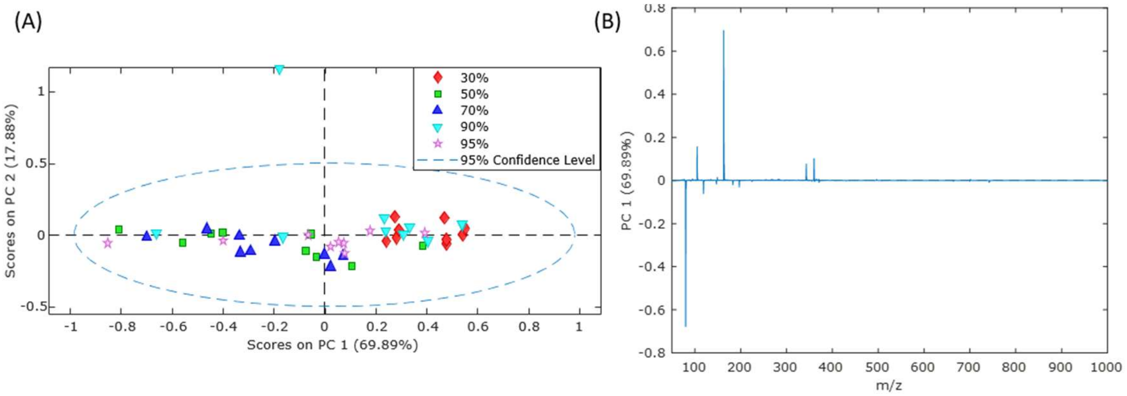

Figure 28. Score plot (A) and loading plot (B) from ANOVA-PCA of weathering degree factor based on the DART-MS spectral data of lighter fluid.

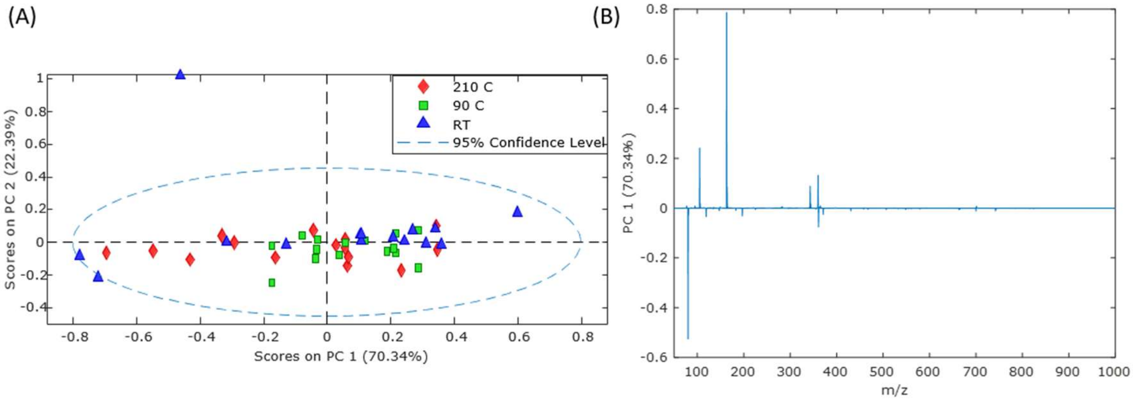

Figure 29. Score plot (A) and loading plot (B) from ANOVA-PCA of temperature degree factor based on the DART-MS spectral data of lighter fluid.

In Figure 30, the peaks at *m/z* 100-400 that were present under the conditions of lower weathering were not present with 90% weathering. This pattern is also seen in the PCA score plot in Figure 31A, where 90% weathering is distinct. The heavy or less-volatile compounds appear on the negative side in the PCA loading plot in Figure 31B.

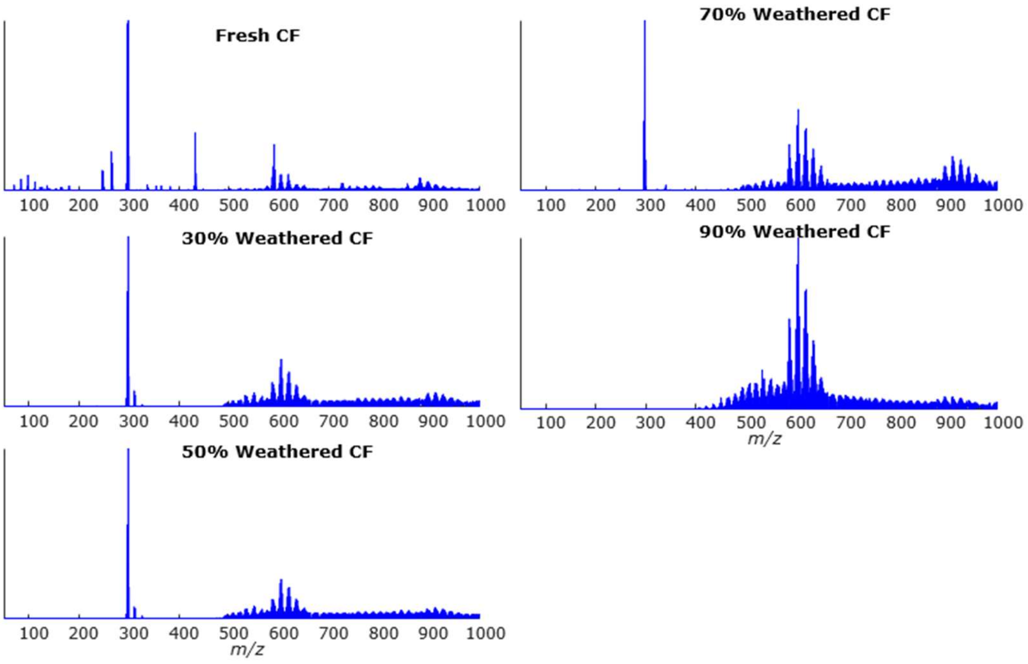

Figure 30. DART-MS spectral variations of charcoal fuel samples affected by the weathering degree factor.

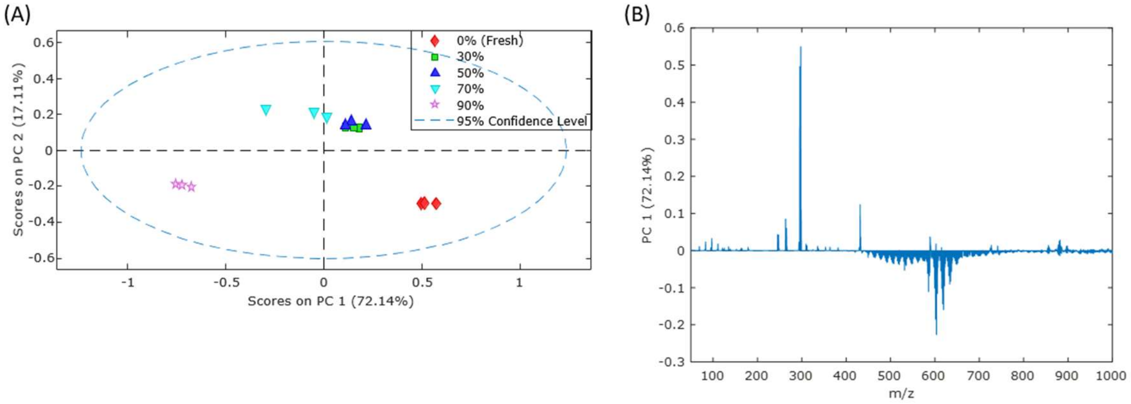

Figure 31. Score plot (A) and loading plot (B) from ANOVA-PCA of weathering degree factor based on the DART-MS spectral data of charcoal fuel.

2.4 Conclusion

The experimental results suggest that both temperature and weathering degree factors should be taken into consideration when preparing the weathered reference IL samples in casework during arson investigations and that analyzing the less volatile components is useful when analyzing ILs because they generally make up most if not all, the remaining components of the ILs after the evaporation of the more volatile compounds. Furthermore, this research demonstrates that although GC/MS has been the conventional analytical method used for analyzing ILs, DART-MS is also a promising method that may yield MS data of high *m/z* range when it comes to profiling the less volatile compounds of some ILs. This study indicates that GC/MS and DART-MS can produce complementary data to profile weathered reference IL samples better than either technique alone.

Section 3. Recovery and Detection of Ignitable Liquid Residues from the Substrates by Solid-phase Microextraction – DART-MS

3.1 Introduction

In arson cases, ignitable liquids (IL) are commonly used to initiate and intensify the fire and are referred to as accelerants [26]. Identifying ignitable liquid residues (ILR) in fire debris on the fire scene provides key evidence to support the possibility of arson. After the extinction of the fire, ILR often exists in low concentrations, and extracting and analyzing them from the fire debris is a challenging step [27]. Since 1990, the American Society for Testing and Materials (ASTM) has provided standard guidelines for fire debris analysis [28]. A critical step in identifying the ILR from the substrates is sample preparation, which converts the ILR into a suitable form for gas chromatography coupled to mass spectrometry (GC/MS) analysis. Several ASTM methods exist for the sample preparations to isolate ILR from the substrate and debris samples. The passive headspace concentration technique using an activated charcoal strip, as described in ASTM E1412-19, is a standard method used by many forensic laboratories in the United States since it is easy to operate and less destructive. In this method, an activated charcoal strip is suspended in the headspace of the sealed heated can for 2-24 hours at 50-80 °C for extraction before the GC/MS analysis [29]. Despite its advantages, this method is time-consuming, and the adsorbed analytes from the charcoal strip must be extracted into carbon disulfide with high toxicity before the GC/MS analysis. Alternative analytical methods circumventing the use of carbon disulfide have been described [29, 30]. Solid phase microextraction (SPME) is an alternative extraction technique first introduced in 1990 by Pawliszyn *et al.*, a simple, rapid, less-destructive sample preparation approach. In fire debris analysis, headspace SPME is commonly used to extract the accelerant from the complex matrices. SPME is a solvent-free extraction technique that generates minute chemical waste. It offers a green analytical approach for characterizing ILRs [31]. The procedures for the use of SPME as a screening method for the IL analysis are outlined in ASTM E2154-15a [32]. Many studies have utilized SPME in ignitable liquid research. Capistran B. A. coupled SPME and rapid-GC/MS techniques to analyze ILR from fire debris samples. Gasoline and diesel fuels were analyzed, and major compounds corresponding to the fuels were identified within 20 min of total workflow time [33]. Another study conducted by Fettig *et al.* describes the extraction of the ILR from fire debris samples using the headspace SPME method followed by the GC/MS analysis. They optimized the experimental parameters and applied the method to analyze complex IL such as gasoline-diesel fuel mixtures and mock burn samples [34]. Similarly, Furton *et al.* utilized SPME with GC/MS to analyze IL and discussed variables, including fiber chemistry, adsorption and desorption temperatures and times, and matrix effects. The results were also compared with those from the ASTM E1412 activated charcoal strip method, and SPME was concluded to be an inexpensive, rapid, and sensitive method for IL analysis [35].

In the studies mentioned above, the SPME was coupled to GC/MS for the analysis of volatile organic components in ILR. The less volatile chemical constituents in the fire debris have received less attention in ILR analysis, which could be critical in supporting the identification of IL. For example, fuel detergents such as polyisobutylene (PIB) succinimides and polyether amines in gasoline and polyethylene glycol (PEG) in paint thinner products were used as marker compounds for the detection of IL, and these polymeric compounds are present at low concentrations and less volatile with high boiling points (>220 °C), making them challenging to be detected with the traditional GC/MS-based strategies [14, 36]. Since the advent of Direct Analysis in Real-Time Mass Spectrometry (DART-MS), it has become a valuable technique in forensics [17] and could serve as an effective approach to support petroleum product analysis [37]. The DART ion source produces a stream of high-energy metastable gas atoms, desorbing and ionizing the molecules of interest. It offers minimal sample preparation, compatibility with various sample matrices, and straightforward data interpretation. Traditionally, DART-MS was considered a screening tool for molecules in less complicated matrix, such as drug analysis. However, with the advancement of sample preparation techniques (*e.g.*, solid phase extraction and SPME), chemometric methods, and mass spectrometric instruments, DART-MS could provide higher discriminatory power in complex matrices and even quantitative results [17]. For example, Khaled *et al.* demonstrated the usefulness of coupling SPME-DART-MS/MS in food safety monitoring applications owing to its high throughput. This study investigated pharmaceutical multiresidue with a wide range of physicochemical properties in beef tissue [38]. Emmons *et al.* evaluated the performance of SPME-DART-MS/MS in screening and quantifying per- and poly-fluoroalkyl substances [39]. Jastrzembski *et al.* demonstrated the rapid trace level analysis of volatile compounds by developing the Solid Phase Mesh Enhanced Sorption from Headspace (SPMESH) method. They utilized this setup for extraction and pre-concentration of volatiles before the DART analysis [40]. In fire debris research, the background signals of complex substrates or matrices often obscure the characteristic ion signals of IL, making it challenging to accurately identify an IL. In the present study, we integrated SPME with DART-MS to study the ILR, and this is the first study, to the best of our knowledge, to implement SPME-DART-MS in IL research. Due to the increasing popularity of DART-MS instrumentation in forensic labs and SPME being a common extraction method for ILR, their synergistic combination could be more easily adopted in the future.

Earlier studies reported the efficiency of DART-MS in detecting the characteristic polymeric compounds in gasoline and paint thinner with complementary chemometric analysis. The DART-MS spectral profiles of gasoline and paint thinner were more robust and not susceptible to variability caused by the weathering process compared to the total ion chromatogram (TIC) profiles from the GC/MS method [14, 36]. A follow-up study [41] analyzed neat IL on substrates (carpet, wood, sand, paper, and soil) by the thermal desorption module and tweezer module of the DART-MS. Firstly, data obtained using thermal desorption provided promising spectral information to distinguish the volatile component region from the fingerprinting region in the gasoline samples and showed immense potential for the analysis of IL and ILR on substrates. However, this study demonstrated the need for an extraction or pre-concentration step to efficiently extract IL from the substrate or debris samples to overcome the matrix effect. The present study aims to develop the SPME-DART-MS method for the detection of ILR on substrates and debris samples and optimize the experimental parameters such as extraction temperature and time for the analysis of gasoline. The substrates (*i.e.*, wood, paper, sand, and fabric) and their debris samples were evaluated to understand the matrix effect in the fire debris analysis. In addition, this strategy was applied to the reanalysis of the ILR debris samples after the initial extraction using the traditional ASTM E1412-19 method. The SPME-DART-MS technique was also tested on paint thinner samples to explore the feasibility of extending its application to other ignitable liquids.

3.2 Materials and Methods

3.2.1 Ignitable Liquids and Material Collection

Gasoline with an 87 octane rating was purchased from a Shell fuel station, and Klean-Strip® Paint Thinner (1 quart) was purchased from local Walmart stores in Murfreesboro, Tennessee. Reagent-grade chloroform was purchased from Fisher Scientific (Pittsburgh, PA). High-point chestnut plank flooring was acquired from a local home improvement store in Murfreesboro, Tennessee. Sea sand was purchased from Merck, Rahway, NJ. Cotton bleached fabric strips were obtained from Testfabrics, Inc., West Pittston, PA. The Marquee multipurpose office paper was used as the paper matrix. The active charcoal strips (8 mm × 20 mm) were purchased from Albrayco Technologies, Inc. (Cromwell, CT). The SPME device and the 7-µm PDMS-coated fused silica fibers on 24-gauge steel needles were purchased from Supelco® Millipore Sigma, St. Louis, MO. The glass vials, phenolic screw hole caps, and septa were purchased from Supelco® Millipore Sigma, St. Louis, MO. The 40-mL glass vial (Catalog number 27184) dimensions are 29 mm × 82 mm × 17 mm (O.D. × H × I.D.), and the screw cap (Catalog number 27187) dimensions are 26 mm ×12 mm (I.D. × H). The tan PTFE/silicone septa (Catalog number 27188-U) are 22 mm in diameter and 0.100 inch thick.

3.2.2 Sample Preparation

For the substrates and charred (debris) substrates analysis, the samples were prepared using paper, wood, and fabric samples with dimensions 2 cm^2 and sand samples weighing 200 mg. Before the extraction, the samples were baked at 150 ℃ for 2 hours to reduce the substrate interferences. The charred substrates were prepared following a modified destructive distillation method used by the National Center for Forensic Science at the University of Central Florida [42]. The substrates were placed in a one-quart metal paint can with six holes of approximately 1 cm in diameter, ignited from the bottom of the can with a propane torch, and burned for 1, 2, 3, or 5 minutes. Heat was applied to the paint can from the bottom with a propane torch at a 4 cm distance from the tip of the flame. Once the smoke appeared, the timer for the burn period began, and after the desired time period, the propane torch was removed. After the burning process, the can was covered with its intact lid and allowed to cool at room temperature. The cooled samples were utilized for the debris analysis [43]. The gasoline samples were prepared by spiking 200 µL of the liquid onto the substrates, and it was left in the fume hood to weather for 2 hours, followed by the SPME extraction at 150 °C for 40 min. During the SPME extraction, the samples were placed into the 40-mL glass vial. The SPME fiber assembly protective steel needle was inserted into the vial and suspended in the sample headspace (Figure 32A). The plunger of the fiber assembly was lowered to allow the protruded PDMS-coated fiber to extract analyte molecules in the ILR headspace under specific temperatures and exposure times. Thereafter, the SPME fiber was retracted and immediately inserted into the T-tube of the DART, so the chemical components from the SPME fiber were desorbed and interacted with the metastable helium gas emitting from the DART source (Figure 32B) at 300 °C for 1 min. Consequently, the ionized molecules entered the inlet of the mass spectrometer for detection. A custom-printed SPME holder was built in the lab using an Original Prusa i3 MK3S+ 3D printer (Prusa Research, Prague, Czech Republic) to secure the SPME device to DART during the sample introduction and to improve the reproducibility of the analysis (Figure 32C).

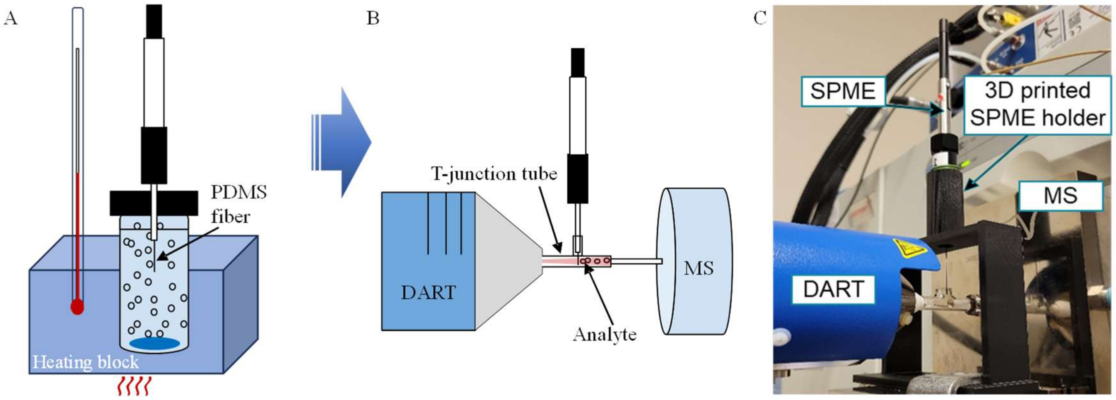

Figure 32. Diagrams of SPME extraction (A), SPME-DART-MS interface (B), and the interface photo (C).

For the ILR reanalysis experiments, paper and sand substrates, along with their charred samples, were tested. The substrate and charred samples with weathered gasoline were placed in the 40-mL glass vial, and an active charcoal strip was inserted into the sample headspace and sealed. The vial was placed in an oven at 60-70 °C for 16-18 h. The activated charcoal strip was extracted in 1 mL of chloroform, followed by the GC/MS analysis of volatile chemical components.

After the charcoal strip was removed, the same glass vial was used to extract the less-volatile chemical components using the SPME method as previously described, which was then analyzed by DART-MS.

3.2.3 DART-MS, DART-HRMS, and GC/MS

The SPME method optimization and substrate/fire debris analyses were performed on a DART ion source (Bruker IonSense, Inc., Saugus, MA) paired with a Thermo LTQ XL mass spectrometer (Thermo Scientific, San Jose, CA). Helium was used as the ionization source with the DART temperature set to 300 °C. The DART was operated in the positive mode, and mass spectra were collected in the *m/z* range of 50-1000. The SPME fiber was directly suspended in the T-junction tube for 1 minute during the analysis. After the analysis, the SPME fiber was cleaned by suspending the fiber again in the T-junction tube until no residual ions were observed.

For the ILR reanalysis experiment, the chloroform extract of the charcoal strip was analyzed on a Shimadzu QP2010S GC/MS with an autosampler by following the Perna *et al.* method [36]. The SPME-DART-MS data was collected on a DART JumpShot® (Bruker IonSense, Inc., Saugus, MA) coupled to a Bruker Compact QTOF-mass spectrometer (Bruker, Bremen, Germany).

3.2.4 SPME Parameter Optimization

This study used a two-factor composite design to evaluate the SPME parameters, such as extraction temperature and time. The experiment was repeated three times at each condition. The full second-order polynomial model was constructed to fit the data, and based on the modeled response surface, optimum conditions were reported.

Equation S1.

$$\boldsymbol{y = b_0 + b_1x_1 + b_2x_2 + b_3x_1^2 + b_4x_2^2 + b_5x_1x_2 + e}$$

The above equation was used to fit the full second-order polynomial model where y is the intensity for the ion of interest; b_{0-5} are the coefficients for the model; x_1 is the extraction time, and x_2 is the extraction temperature.

3.2.5 Evaporation of Gasoline on Wood Matrix

This experiment was conducted to study the correlation between the percentage of gasoline that remained on the substrate (wood) with time. A small wooden piece (approximately 1 cm^2) was used as a substrate, and its initial weight was recorded at the beginning of the experiment. A 200 µL of gasoline was spiked onto the wood, and the weight change of the wooden piece was recorded at 0 min, 1 min, 5 min, 10 min, 30 min, 1 h, 2 hrs, 4hrs, 24 hrs, and 48 hrs. This experiment was conducted in triplicates on an analytical balance (Mettler Toledo ME204E, Columbus, OH). The gasoline percent decrease was calculated from the experimental values, and the percent gasoline remained on the wood was calculated and plotted against time.

3.2.6 Sensitivity Comparison Between the Thermo LTQ XL and Bruker QTOF MS

To evaluate the instrumentation sensitivity, the gasoline samples were prepared with different dilution factors, such as 10, 50, 100, and 200. A 10 × gasoline diluted sample was prepared by adding 100 µL of gasoline into 900 µL of chloroform solvent to achieve a final volume of 1 mL. The 50 × sample was prepared by spiking 20 µL of gasoline into 980 µL of chloroform solvent, and 100 × was prepared by spiking 10 µL of gasoline in 990 µL of chloroform solvent. Similarly, the 200 × gasoline samples were prepared by spiking 5 µL of gasoline into 995 µL chloroform solvent. The prepared samples were analyzed in triplicates on Thermo LTQ XL and Bruker QTOF mass spectrometers by utilizing the QuickStrip^{TM} module; the DART temperature was set to 400 °C, helium gas was used as the ionization source, and the instrument operational parameters mentioned by Barnette *et al.* were followed. [14]. The ions at *m/z* 284.5, 474.5, 530.5, and 586.5 were monitored to identify gasoline. Using the Thermo LTQ XL mass spectrometer, the 10 × diluted gasoline showed a clear gasoline profile exhibiting all the characteristic ions, whereas, in the 100 × dilution, not all the *m/z* ions were clearly observed due to their low ion intensities. For the Bruker QTOF analysis, the initial dilution was started with 50 ×, and the characteristic ions of gasoline were clearly observed at 100 × dilution; after the background subtraction, the *m/z* gasoline characteristic ions were observed with an intensity of 10^4.

3.2.7 Data Analysis

For the DART-MS data processing, the average mass spectrum of 60 scans (0.17 min) for each sample was exported to Excel with Xcalibur 2.1 software (Thermo Scientific, Waltham, MA) after subtracting the background. The data sets were binned by mass-to-charge ratios from 50 to 1000 Da with 0.5 Da increments. The statistical analysis was conducted using MATLAB R2021a (MathWorks Inc., Natick, MA).

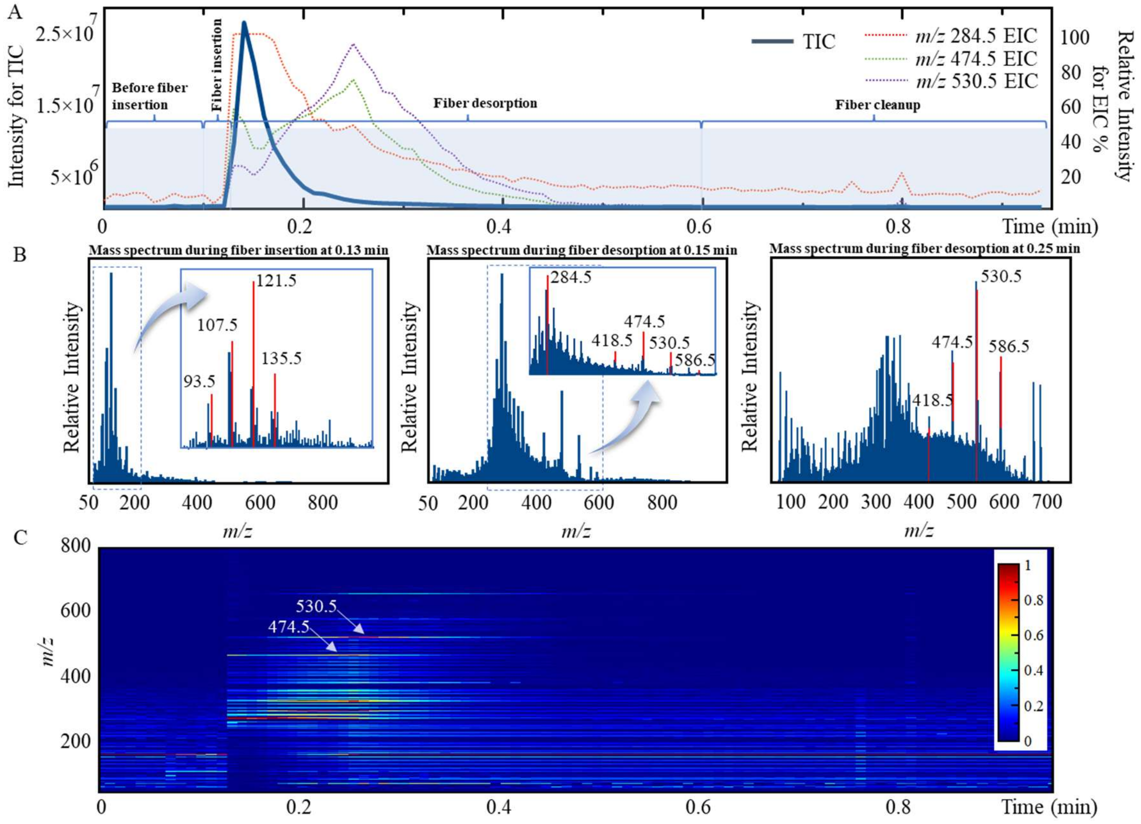

Figure 33. A representative SPME-DART-MS data for gasoline residues on a sand sample: A, total ion chronogram (TIC) and extracted ion chronograms (EIC) of characteristic ions; B, representative mass spectra during the SPME fiber insertion and desorption process with characteristic ions labeled in red; C, a display of raw data in a heat map with ion intensity normalized to maximum intensity.

3.3 Results and Discussion

3.3.1 Identification of Gasoline by SPME-DART-MS Method

An example of SPME-DART-MS data for gasoline residue detection from sand substrates is shown in Figure 33. After the SPME extraction, the fiber was inserted into the DART helium gas stream for desorption for 1 min. During this process, when the SPME fiber interacted with the heated metastable gas atoms, the desorption and ionization of analytes took place. The chronograms were arbitrarily divided into four regions, and the mass spectra from corresponding areas were discussed as follows. Figure 33A shows the TIC and EIC for selected characteristic ions for gasoline, including *m/z* 284.5, 474.5, and 530.5 at different desorption phases during the DART analysis. Before the fiber insertion, the background mass spectra were examined and recorded to ensure the absence of contamination and for the background subtraction. At the moment of the fiber insertion into the T-tube of the DART-MS, the TIC peak arose. The mass spectra from the first 2-3 seconds of the fiber insertion significantly differed from those in the following scans during the desorption process. Figure 33B shows the mass spectra with the zoomed views depicting the *m/z* ions at fiber insertion and desorption phases. The dominance of low *m/z* ions 93.5, 107.5, 121.5, and 135.5 was observed at the fiber insertion phase at 0.13 min, illustrating the desorption of volatile components from the SPME fiber. During the fiber desorption phase, the SPME fiber had been exposed to the stream of hot metastable He atoms for a longer period, which led to the desorption of higher *m/z* ions such as 474.5 and 530.5 at 0.15 min corresponding to the less volatile compounds. At 0.25 min, the *m/z* 474.5, 530.5, and 586.5 ions were distinctly spotted, and their intensities decreased to the baseline in the fiber desorption phase. The EIC of each ion in Figure 33A depicts the trend in intensity during the fiber desorption. For example, the *m/z* 284.5 intensity was higher during the fiber insertion phase, whereas its intensity decreased during the fiber desorption phase. As a comparison, *m/z* 474.5 and 530.5 ion intensities were higher during the fiber desorption phase, and their intensities decreased as the desorption time progressed. All the ions reached baseline levels after 30 seconds, but the SPME fiber was kept in the DART gas stream for another 30 seconds to achieve complete cleanup and be ready for the subsequent sample extraction. The *m/z* 93.5, 107.5, 121.5, and 135.5 have a repeating unit of 14 Da, which could correspond to the $–CH_2$ group. Our previous study reported that *m/z* 284.5, 474.5, 530.5, and 586.5 represented the gasoline characteristic ions. They have a repeating unit of 56 Da that corresponds to isobutylene ($–CH_2–C(CH_3)_2–$, 56.0626 Da) [14]. The samples were also analyzed using the DART-QTOF-MS instrument to identify the characteristic ions. The accurate masses of the characteristic ions were measured to be 284.2953, 418.4046, 474.4676, 530.5301, and 586.5928. The *m/z* 284.2953 was identified to be the protonated octadecanamide with the ionic formula $[C_{18}H_{37}NO + H]^+$, with mass accuracy and isotopic pattern fit factor (mSigma) of -1.7 ppm and 7.2, respectively. Octadecanamide is commonly used as a corrosive inhibitor in oil wells with a boiling point of 250 °C [44]. Hence, it was not surprising to identify it in gasoline products. Similarly, the ion series *m/z* 418.5, 474.5, 530.5, and 586.5 were determined to correspond to the polyisobutylene succinimide (PIBS), and the chemical structures of PIBS were proposed based on the HRMS spectral data and previous literature [45], as shown in Table 8. Hence, our result indicates that the SPME-DART-MS method is effective in recovering and detecting the less volatile compounds in the gasoline residues. Figure 33C is the heat map of a three-dimensional representation of the data matrix from the SPME-DART-MS analysis, showing the complexity of chemical components from the SPME extract. Despite the characteristic ions discussed above, a cluster of unresolved ions, primarily in the *m/z* 200-400 range, was found in the mass spectra during desorption. They could be attributed to organic matter in the sand matrix containing the elemental composition of CHO, CHOS, CHON, and CHONS compound classes. However, decoding the chemical structure of organic matter remains a challenging analytical task. The presence of heterocyclic compounds in petroleum products, including gasoline, provides opportunities for the use of the DART technique to impart greater specificity of ILR identification via these compounds with their electronegative oxygen, nitrogen, and sulfur atoms and higher proton affinities to yield distinctive $[M+H]^+$ ions [46].

Table 8. Tentative Identification of Selective Characteristic Ions for Gasoline

Measured *m/z*	Ion Formula	Theoretical *m/z*	Mass Accuracy (ppm)	Structure
284.2953	$[C_{18}H_{37}NO+H]^+$	284.2948	-1.7	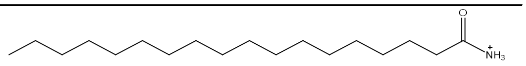
418.4046	$[C_{28}H_{51}NO+H]^+$	418.4043	0.6	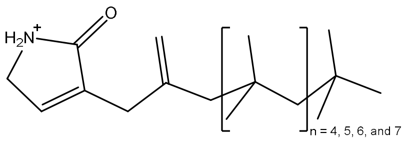
474.4676	$[C_{32}H_{59}NO+H]^+$	474.4669	1.4	
530.5301	$[C_{36}H_{67}NO+H]^+$	530.5295	1.1	
586.5928	$[C_{40}H_{75}NO+H]^+$	586.5921	1.1	

The SPME extraction was extended to paint thinner to evaluate the applicability of this construct to other ignitable liquids. Figure 34 depicts the TIC of paint thinner on the sand sample with the respective averaged mass spectrum. Our previous study elucidated the presence of two groups of the ions: *m/z* 195, 239, 283, 327, 371, 415, and 459 corresponding to the PEG oligomers and *m/z* 613, 641, 669, 697, 725, 753, and 781 corresponding to polymeric compounds with alkyl chains in the paint thinner samples by Quickstrip™ DART-MS [36]. Most of the reported characteristic ions were also identified in the paint thinner on the sand sample from the SPME-

DART-MS analysis, except some of the ions corresponding to PEG were missing due to the interference of the organic matter in the sand matrix. Similar to the gasoline analysis, a group of ions in the low mass range (*i.e.*, *m/z* 83, 97, 119, 133, 147, *etc.*, in Figure 34) was observed immediately after the insertion of SPME fiber into the DART gas stream and completely desorbed rapidly. It is worth noting that these ions were not detected when the paint thinner or gasoline was analyzed by the Quickstrip™ DART-MS method [14, 36]. One possible reason for this difference was that DART ionization (*i.e.*, the positive mode used in this experiment primarily based on Penning ionization and proton transfer) favors the molecules such as fuel additives and PEG; in contrast, the low molecular-weight volatile organic compounds (VOC) in petroleum products (primarily hydrocarbons) were more challenging to ionize under positive mode. Therefore, all the compounds were present and ionized together when the Quickstrip™ module was employed, and the ionization competition suppressed the signals of VOC, resulting in the mass spectrum being dominated by fuel additives and PEG peaks. The desorption temperatures required for VOC and PEG or PIBS from SPME were different, which provided a separation between the two groups of compounds so that the VOC could be desorbed earlier and detected with less ionization competition and enabled the inclusion of additional characteristic ions for VOC for the detection of gasoline or paint thinner in the samples. Similar results were also reported when thermal desorption DART-MS was employed where the clusters of ions in the low mass range between *m/z* 70-180 were detected in gasoline, paint thinner, kerosene, etc., at lower desorption temperature (i.e., 25-100 °C). In contrast, the less volatile compounds were detected at elevated temperature (i.e., 300 °C or higher for gasoline) [41]. In addition to the characteristic ions for gasoline or paint thinner mentioned above, another cluster of ions with *m/z* higher than 800 and 74 Da repeating unit ($-Si(CH_3)_2O-$) were observed sometime in the SPME-DART-MS spectrum, which corresponded to the PDMS on the fiber (Figure S1). Due to their unique mass spectral pattern and relatively low intensity, they did not interfere with the detection of characteristic ions for gasoline or paint thinner.

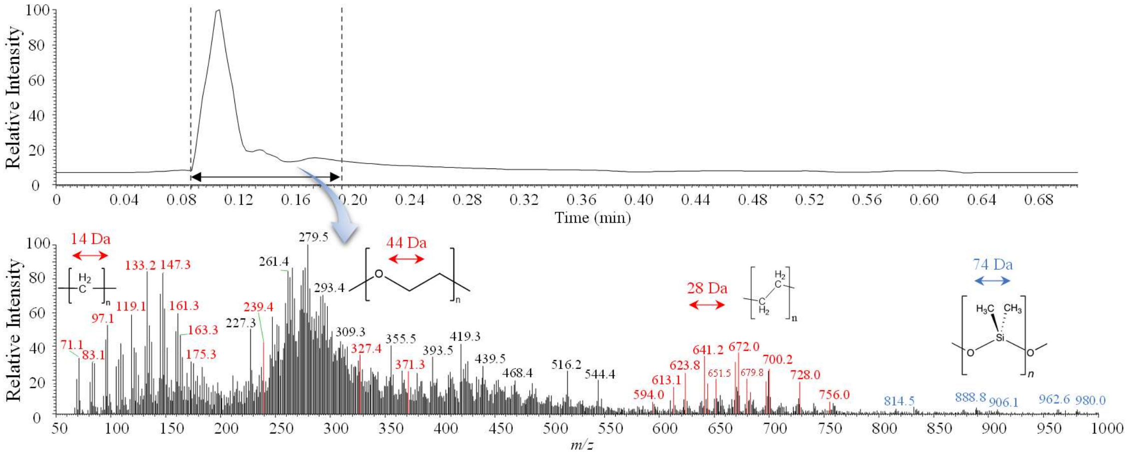

Figure 34. A representative SPME-DART-MS data for paint thinner residues on a sand sample TIC (top) and averaged mass spectrum after subtracting the background spectrum from 0-0.04 min (bottom).

3.3.2 Optimization of SPME Parameters

In the SPME extraction process, the two correlated factors of temperature and time are crucial in the extraction effectiveness. The classical design of experiment methods was commonly applied to evaluate and optimize the experimental parameters [27]. Among different types of response surface designs (RSD), the two-factor central composite design (CCD) was used in this study [47]. Various levels were chosen for the extraction temperature and time factors, and the obtained data was used to fit the full second-order polynomial models, as shown in Figure 35A. The optimization experiment was conducted without the presence of substrates. In short, 100 µL of liquid gasoline was spiked onto the vial and weathered 2 h in the fume hood. Subsequently, the vial is sealed for the SPME extraction under the condition shown in Figure 35A, followed by the DART-MS analysis. All the experiments were carried out in triplicates. The intensity for the ions of interest were extracted from the data matrix and modeled. Examples of the contour plots of the modeled response surface for *m/z* 284.5 and 474.5 are shown in Figure 35B. The optimum extraction result for *m/z* 284.5 occurs at an extraction temperature of 150 °C for 40 min with the highest ion intensity. Similarly, *m/z* 474.5 ion intensity was relatively high at 150 °C with an extraction time of 40 min compared to the results at lower temperatures. To achieve the optimum extraction result for *m/z* 474.5, a higher temperature than 150 °C is needed. As discussed in the previous section, desorbing PIBS from SPME fiber takes longer than desorbing octadecanamide, indicating a lower volatility. The SPME extraction optimization results agreed with this observation, and higher extraction temperature would favor the less volatile compounds such as PIBS. The ion intensity for *m/z* 474.5 at 40 min and 150 °C is about 72% of the best extraction condition at 30 min 180 °C. However, the higher extraction temperature would result in decreased extraction efficiency for *m/z* 284.5 and more significant interference from some substrates such as sand and fabric. Based on the results, the SPME conditions were chosen at 150 °C for 40 min for extracting the residues for this study.

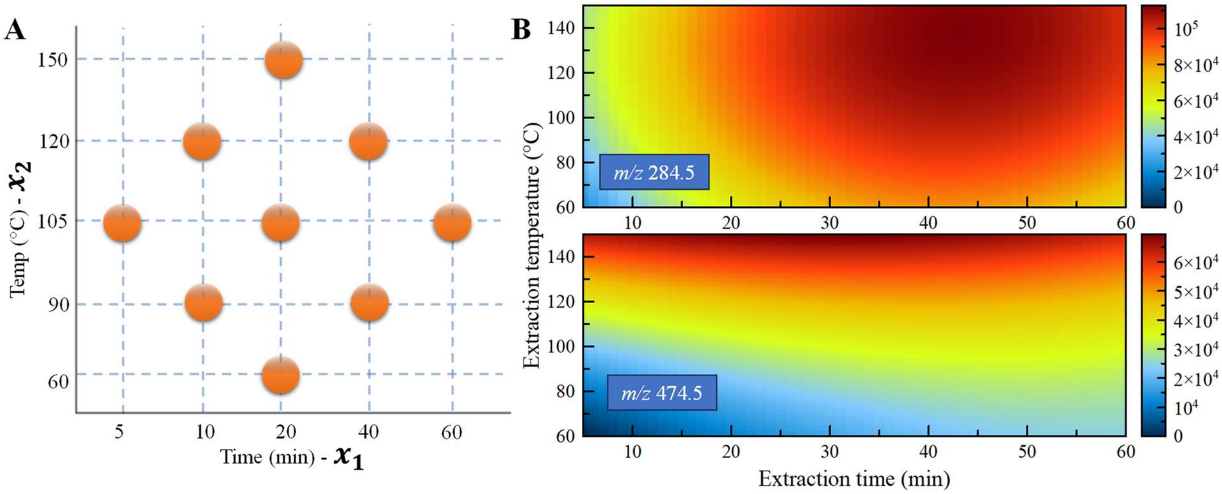

Figure 35. A central composite design (A) and response surface of the second-order polynomial models for characteristic ions *m/z* 284.5 and *m/z* 474.5 (B).

3.3.3 Analysis of Gasoline Residues on the Substrates and Fire Debris

In the ILR analysis, the substrate matrix often interferes with the identification of ignitable liquid used to commit the arson crime. Table 9 depicts the analysis of gasoline on DART-MS using different sampling modules. This table compares the results obtained from the SPME-DART-MS analysis with the other DART-MS methods, such as direct insertion using a capillary tube and Quickstrip™ module. In the latter two methods, maximum numbers of characteristic ions corresponding to the less volatile fuel additive compounds in gasoline were observed, such as *m/z* 284.5 for the protonated octadecanamide and the ions in the higher mass range, including *m/z* 474.5, 530.5, 586.5, 642.5, 698.5, 754.5, 810.5, and 866.5 with the repeating units of 56 Da. In the previous study, the fingerprinting region of the gasoline has shown the presence of *m/z* 284.5, 474.5, 530.5, 586.5, 642.5, 698.5, 754.5, 810.5, *etc.* [14], which matches with the results obtained from the capillary and Quickstrip™ methods. The ions in the low mass range, such as *m/z* 93.5, 107.5, 121.5, and 135.5 with repeating units of 14 Da, were not detected from the capillary and Quickstrip^{TM} methods due to the ionization competition as explained in Section 3.3.1. The liquid gasoline residues were extracted by SPME and analyzed on DART-MS, and the results showed the presence of *m/z* 93.5, 107.5, 121.5, 135.5, 284.5, 474.5, 530.5, 586.5, 642.5 and 698.5, which match with the gasoline characteristic ion pattern. Similarly, the SPME-DART-MS analysis on the substrates and fire debris has shown the presence of various ions corresponding to the gasoline residues. The gasoline residues on the substrates, such as paper, sand, wood, and fabric, have shown the presence of low *m/z* ions in almost all sample replicates. The *m/z* 93.5, 107.5, 121.5, 135.5, 284.5, 474.5, 530.5, and 586.5 were observed in all the substrate samples except for the fabric matrix in which *m/z* 530.5 was unresolved due to the interference of the polymeric backbones in the fabrics. The *m/z* 698.5 was not detected in any substrate samples, and *m/z* 642.5 was only observed from the paper substrate. As a polymeric compound, the PIBS follows the general trend: the increase in the polymer chain length leads to decreased volatility as larger molecules require more energy to overcome intermolecular forces and evaporate. Therefore, the polymeric units corresponding to *m/z* 642.5 or 698.5 or larger would require higher temperatures to be extracted and detected by SPME-DART-MS. The fire debris samples prepared from paper, sand, fabric, and wood have shown the presence of the low *m/z* ions 93.5, 107.5, 121.5, and 135.5, and also the ions from the fingerprinting region such as *m/*z 284.5, 474.5, 530.5 and 586.5 in most of the samples. Unlike the unburned fabric substrate, mass spectra from the debris samples have shown more gasoline-specific ions in the DART analysis. This could be because the polymers in the fabric could have been degraded by the heating during the debris sample preparation. Overall, the SPME-DART-MS analysis on the substrates and fire debris yielded most gasoline characteristic ions lower than *m/z* 700.

Table 9. Observation of gasoline characteristic ions from different DART-MS experiments

Sample Type		Shell Gasoline Characteristic Ions (*m/z*)										
		<150	284.5	474.5	530.5	586.5	642.5	698.5	754.5	810.5	866.5	923.5
Literature[12,19]			+	+	+	+	+	+	+	+	+	+
Capillary DART-MS (Liquid gasoline)	R1	+	+	+	+	+	+	+	+	+	+	+
	R2	+	+	+	+	+	+	+	+	+	+	+
	R3	+	+	+	+	+	+	+	+	+	+	+
Quickstrip™ DART-MS (Liquid gasoline)	R1		+	+	+	+	+	+	+	+	+	+
	R2		+	+	+	+	+	+	+	+	+	+
	R3		+	+	+	+	+	+	+	+	+	+
SPME DART-MS (No substrates)	R1	+	+	+	+	+	+	+				
	R2	+	+	+	+	+	+	+				
	R3	+	+	+	+	+	+	+				
SPME DART-MS (Gasoline on paper)	R1	+	+	+	+	+	+					
	R2	+	+	+	+	+	+					
	R3	+	+	+	+	+	+					
SPME DART-MS (Gasoline on sand)	R1	+	+	+	+	+	+					
	R2	+	+	+	+	+	+					
	R3	+	+	+	+	+						
SPME DART-MS (Gasoline on fabric)	R1	+	+	+		+						
	R2	+	+	+		+						
	R3	+	+			+						
SPME DART-MS (Gasoline on wood)	R1	+	+	+	+	+						
	R2	+	+	+	+	+						
	R3	+	+	+	+	+						
SPME DART-MS (Gasoline on paper debris)	R1	+	+	+	+	+	+					
	R2	+	+	+	+	+						
	R3	+	+	+	+	+						
SPME DART-MS (Gasoline on heated sand)	R1	+	+	+	+	+						
	R2	+	+	+	+							
	R3	+	+	+	+							
SPME DART-MS (Gasoline on fabric debris)	R1	+	+	+	+	+	+	+				
	R2	+	+	+	+	+	+	+				
	R3	+	+	+	+	+	+	+				
SPME DART-MS (Gasoline on wood debris)	R1	+	+	+	+	+	+	+				
	R2	+	+	+	+	+						
	R3	+	+	+	+	+	+	+				

3.3.4 Pattern Matching Based on Characteristic Ions

The receiver operating characteristic curve (ROC) analysis was first developed in the 1950's with electronic signal detection theory. Initially, this method was employed in World War

II for radar signal screening to distinguish between the signal (true positive result) and noise. Eventually, this method was used in other fields, such as psychology, medicine, and machine learning [48, 49]. In this study, the ROC curve is utilized to accurately determine the presence of gasoline residue based on the characteristic ions by measuring the sensitivity (true positive) and specificity (true negative). A total of 306 mass spectra were tested, which included data collected from the SPME-DART-MS experiment for gasoline and paint thinner with and without substrate/debris in this study and the spectra from the Quickstrip^{TM} DART-MS for various fresh and weathered IL (such as gasoline, paint thinner, torch fuel, lighter fluid, Japan drier, and diesel) in our previous study [36]. Since the ions in the low mass range, such as *m/z* 93.5, 107.5, 121.5, and 135.5, were generally not detected by Quickstrip^{TM} DART-MS, they were not evaluated in this section. ROC was created by plotting the "sensitivity" to the "1-specificity" at various decision thresholds, defined by the number of characteristic ions for gasoline in Table 9 observed in the mass spectrum. For example, if the threshold was arbitrarily chosen to be 4 ions, the detection of 4 or more characteristic ions was determined as "identification," otherwise as "inconclusive." The sensitivity was obtained by dividing the sum of true positive outcomes by the total positive instances (or true positive rate). The "1-specificity" was calculated by dividing the sum of false positives by the total of negative instances (or false positive rate). The area under the curve (AUC) was derived from ROC analysis as an accuracy metric, for which values above 0.9 indicate a 'rather high' discrimination accuracy. As shown in Figure 36A, decreasing the criterion (i.e., using fewer characteristic ions as a threshold) for the identification causes it to slide upward and to the right along the curve, as the rate of true positive identification and false positive identification both increases. A stricter threshold increases the false negative rate, making the method less sensitive to gasoline residue detection. The AUC in this plot is 0.985, which indicates the method is discriminative and is expected to have good detection performance for gasoline identification. Figure 36B illustrates that as the number of ions for gasoline identification increases, the specificity of gasoline identification increases, and the sensitivity decreases. When four characteristic ions were selected as the threshold, the true positive rate was 92.0%, and the true negative rate was 95.2%, which was considered optimal in this analysis (slightly favored the specificity to minimize the risk of wrongful convictions in arson cases). Based on this evaluation, the four most discriminative ions for gasoline identification were found to be *m/*z 284.5, 474.5, 530.5, and 586.5.

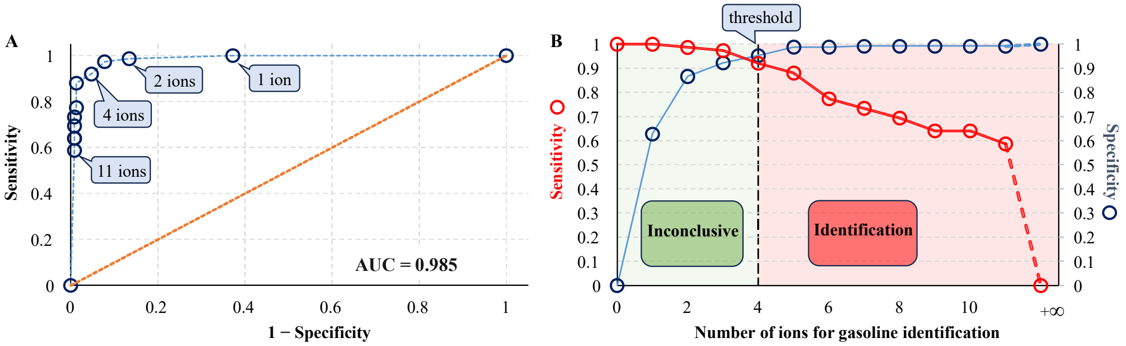

Figure 36. ROC curve (A) and the sensitivity/specificity plot (B) for gasoline identification.

As discussed in Section 3.3.1, the characteristic ions for gasoline were detected at different SPME thermal desorption stages. Therefore, the data from SPME-DART-MS would be better examined scan-by-scan to reach the correct outcome, minimizing false identification and false exclusion. In addition, the characteristic ions of gasoline were usually detected as patterns of 14 Da difference for low mass range and 56 Da difference for fuel additive (Figure 33). The detection of only one ion from each ion cluster should not be considered sufficient evidence for the identification due to the possible interference from other sources. An in-house MATLAB script was used to create mass spectral figures with characteristic ions highlighted for gasoline or paint thinner to assist in the comparison. For example, for gasoline identification, the characteristic ions were labeled red (Figure 37A). The mass spectrum from the gasoline residue on the fabric debris sample (Figure 37A middle) contains three resolved characteristic ions for fuel additive and *m/z* 284.5 with supporting ions in the low mass range, so identification was concluded. One gasoline characteristic ion was also observed in the mass spectrum from the paint thinner residue on the fabric debris sample (Figure 37A right), but no other resolved characteristic ions were identified, so a negative identification of gasoline was concluded on this sample. A similar process was conducted for paint thinner identification for the same mass spectral data, and the correct identification and exclusion were achieved (Figure 37B).

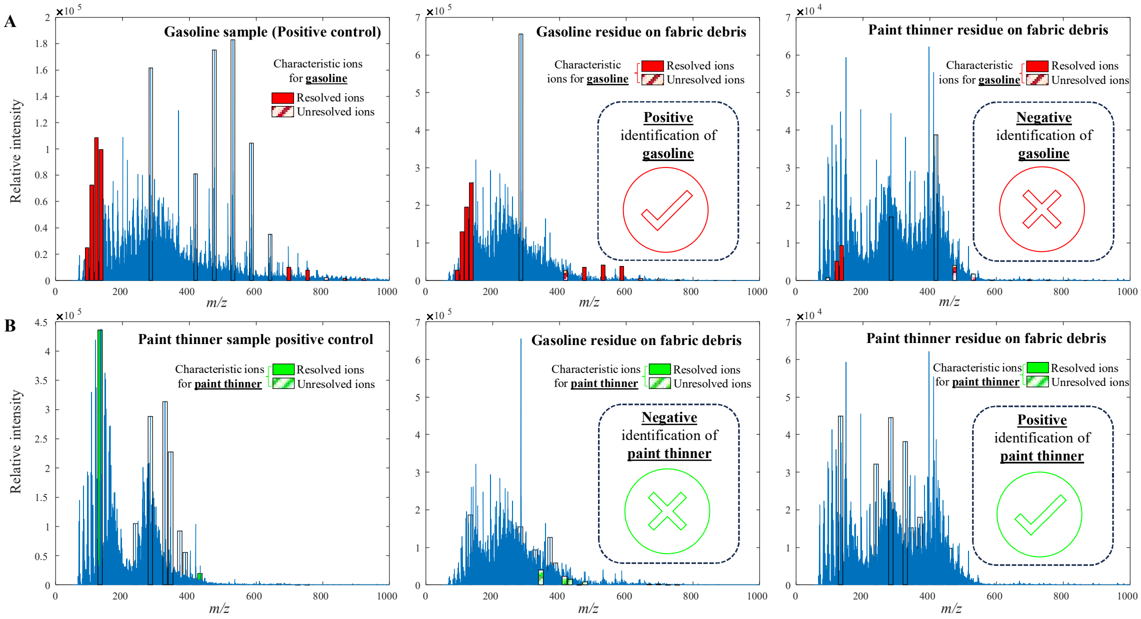

Figure 37. Comparison of mass spectra between positive control samples and IL residue on fabric debris samples for gasoline identification (A) and paint thinner identification (B). Resolved ions refer to characteristic ions (*m/z* of M) with intensity at least 50% higher than their neighboring ions (*m/z* of M−1 or M+1); otherwise, they are considered unresolved ions.

3.3.5 Evidence Reanalysis by SPME-DART-HRMS after ASTM E1412 Method

In the United States, the ILR in fire debris samples in forensic laboratories was primarily prepared by the ASTM E1412 passive headspace concentration with the activated charcoal method [29] and analyzed by the ASTM E1618 GC/MS method [50]. One of our hypotheses is that the low extraction temperature (i.e., 50-80 °C) in the ASTM E1412 method would not effectively extract the less volatile compounds, such as fuel additives, from ILR, and the fire debris samples could be reanalyzed by our SPME-DART-MS method to provide complementary information to support the identification of ILR. In this section, gasoline on the paper and sand substrates and their debris samples were tested. The samples were first extracted by placing a piece of active charcoal strip in the headspace and extracting for 16-18h at 60-70 °C in the oven. Subsequently, the active charcoal strip was extracted by chloroform with subsequent GC/MS analysis to identify volatile compounds. Figure 38 shows the GC/MS TIC profiles from gasoline on paper debris samples after the passive headspace extraction with activated charcoal. The peaks for toluene, ethylbenzene, *m,p,o*-xylenes, 1,2,4-trimethylbenzene, indane, and naphthalene were identified in the TIC profile. The SPME fiber was inserted into the same sampling vial to extract the less/non-volatile chemical components by following the condition optimized in Section 3.3.2. The SPME fiber was placed in the DART helium stream for desorption and ionization, and the ions were detected by a Bruker QTOF mass spectrometer. For this experiment, the DART-QTOF instrument was chosen for its higher sensitivity, mass accuracy, and mass resolution. The mass spectrum obtained for this analysis clearly showed the presence of *m/z* 284.2953, 474.4676, 530.5301, and 586.5928, corresponding to gasoline characteristic ions. Table 10 summarizes the presence of gasoline characteristic ions from different substrate and debris samples. The paper and its debris samples have shown the presence of gasoline characteristic ions more distinctly than the sand and debris samples. The results indicate that the fire debris samples could be reused for the analysis of the less volatile compounds by DART-MS after being extracted by headspace activated carbon strip under low temperature (ASTM E1412 method), which could significantly enhance their evidentiary value. This strategy could also be used to reanalyze the archived fire debris evidence from the cases with inconclusive results. The ability to detect the less volatile compounds in IL in fire debris could have great forensic significance for arson investigation cases, which can help identify or narrow down the list of candidate ILs. The conventional GC/MS method is still the gold standard for IL analysis in forensic labs, but the DART-MS data of less volatile components and heterocyclic compounds containing nitrogen and sulfur from the same fire debris evidence would provide complementary information to the conventional GC/MS method.

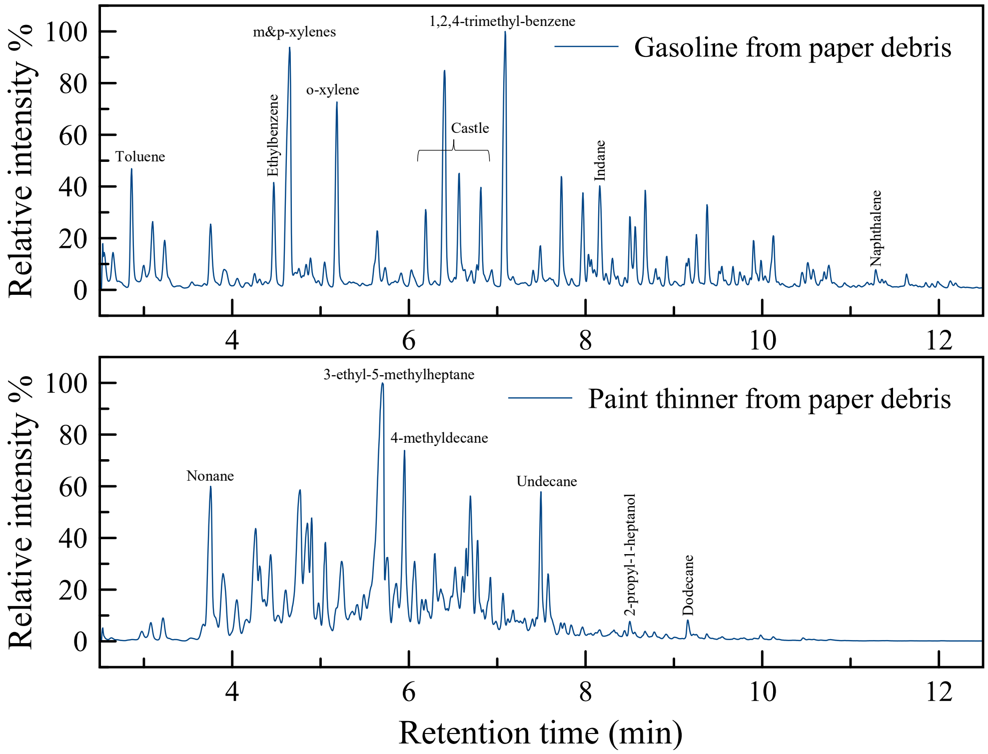

Figure 38. TIC profiles from GC/MS analysis for gasoline and paint thinner on paper debris samples after the passive headspace concentration with activated charcoal extraction.

Table 10. Observation of Shell gasoline characteristic ions from DART-HRMS experiments

Sample Type		Gasoline Characteristic Ions (*m/z*)							
		284.5	474.5	530.5	586.5	642.5	698.5	754.5	810.5
SPME DART-MS (Gasoline on paper)	R1	+	+	+	+	+	+	+	+
	R2	+	+	+	+	+	+	+	+
	R3	+	+	+	+	+	+	+	+
SPME DART-MS (Gasoline on sand)	R1	+	+	+	+	+	+	+	
	R2	+	+	+	+	+	+		
	R3	+	+	+	+				+
SPME DART-MS (Gasoline on paper debris)	R1	+	+	+	+	+	+	+	+
	R2	+	+	+	+	+	+	+	+
	R3	+	+	+	+	+	+	+	
SPME DART-MS (Gasoline on sand debris)	R1	+	+	+	+	+	+	+	+
	R2	+	+	+	+				
	R3	+	+	+	+	+	+	+	

3.3.6 Limitations

It is important to acknowledge the limitations of the SPME-DART-MS method for ILR detection presented in this study. Manual SPME extraction and desorption introduced variability to the experiment. One of the predominant sources of variations in the experimental results was the position of SPME fiber in the DART helium gas stream for desorption. A custom-printed SPME holder was used to help secure the SPME sampling syringe and ensure a fixed depth of SPME fiber in the gas stream and a constant distance to the exit of the DART ceramic cap during the desorption process (Figure 32) to significantly improve the reproducibility of the results. However, special care was needed while transferring the SPME from extraction to desorption and exposing SPME fiber at the optimal position for desorption should be completed as quickly as possible to prevent the loss of analytes. The time-consuming SPME extraction step limits the overall analysis throughput. Implementing an autosampler for SPME-DART-MS would be beneficial for enhancing the reproducibility and throughput of this method. The heated metastable helium from DART was used as the desorption gas for SPME, but it had a negative impact on the usable lifespan of SPME fiber. In this study, the SPME fiber was replaced with a new fiber after about 50 extractions. The detection limits of GC/MS-based ASTM methods are stated as 0.1 µL of neat gasoline from a sample, which is typically evaluated immediately right after spiking the gasoline sample [51]. Our SPME-DART-MS analysis focused on the less volatile compounds, such as fuel additives in gasoline, which are generally present at low concentrations (<0.5%, w/w) in gasoline samples [14]. The amount of volatile organic compounds in gasoline can be reduced significantly due to evaporation. For example, after spiking 100 µL of gasoline onto the wood sample, the weight loss in gasoline with time was plotted in Figure 39. It is observed in the first 5 min, closer to the 33 ± 1% of the sample was lost. In 2 hours, only 15 ± 2% of the gasoline was retained on the wood sample. The gasoline samples in this study were prepared after weathering for at least 2 hours in the fume hood, which is a simulation of ILR samples. Another important factor for the sensitivity and selectivity of the method is the type of mass spectrometer used. The majority of this study was conducted with the ion trap MS with unit mass resolution. When the QTOF MS was used, a ten-fold sensitivity enhancement for the detection of fuel additive ions in gasoline was observed, and the high accuracy and high-resolution mass spectra reduced the ambiguity of the detection, especially when complex substrates were involved. Lastly, the GC/MS method has shown superior resolving power to detect various volatile organic compounds in ILs, which is critical for distinguishing different types of ILs. In contrast, the DART-MS method cannot offer sufficient information to classify the ILs into the ASTM classes because of its limited speciation capability for alkanes and aromatics. However, DART-MS spectral profiles could aid in the further characterization of IL by providing data for less volatile chemicals, such as ion clusters for fuel additives, and this information should be considered orthogonal to the GC/MS data, which can complement the existing GC/MS method for identifying ILs.

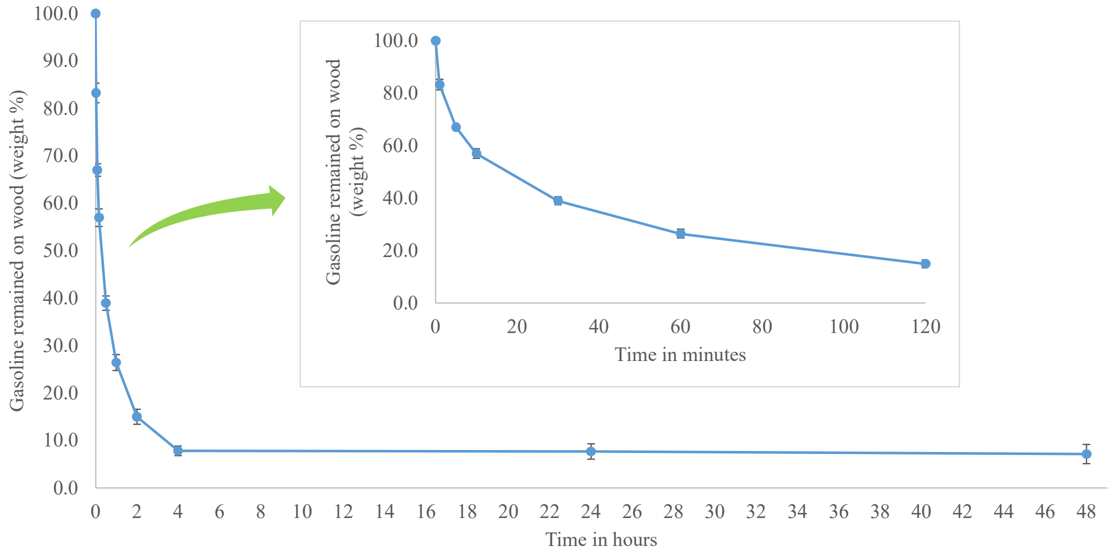

Figure 39. The time series experimental plot shows the rate of decrease of gasoline mass on wood by plotting evaporation time on the X-axis and weight percent remaining on the Y-axis. The inset plot shows time in minutes on the X-axis, and weight percent remains on the Y-axis.

3.4 Conclusions

In this study, we have shown the application of the SPME-DART-MS setup in the analysis of ILR (gasoline and paint thinner) from substrates and fire debris matrices. This method could be utilized to recover and detect the volatile and less volatile marker compounds of ILR. The DART ionization technique is conducive to the analysis of oxygen- and nitrogen-containing compounds at trace levels due to their higher proton affinities relative to the gasoline hydrocarbons present at significantly higher levels. The results of the second-order polynomial models for the optimization of SPME extraction indicate that a high temperature (120-150 °C) was required to extract less volatile compounds. The characteristic ion patterns of gasoline residues in the low-to-mid mass range (< *m/z* 700) matched well with the liquid samples directly analyzed by DART-MS. The desorption of ILR on SPME fiber was achieved by inserting the fiber into the DART-MS helium gas stream under 400 °C for 1 min, and no carry-over residues were observed. This method also successfully reanalyzed the debris samples after using the traditional activated charcoal strip extraction. Future studies will apply the SPME-DART-MS method to other ignitable liquids and investigate the effects of burning conditions.

References

[1] M. Baron, FORENSIC SCIENCES | Arson Residues, in: P. Worsfold, A. Townshend, C. Poole (Eds.), Encyclopedia of Analytical Science (Second Edition), Elsevier, Oxford, 2005, pp. 365-372.

[2] M. Ferreiro-González, G.F. Barbero, M. Palma, J. Ayuso, J.A. Álvarez, C.G. Barroso, Determination of Ignitable Liquids in Fire Debris: Direct Analysis by Electronic Nose, 16(5) (2016) 695.

[3] T.J. Bruno, S. Allen, Weathering Patterns of Ignitable Liquids with the Advanced Distillation Curve Method, J Res Natl Inst Stand Technol 118 (2013) 29-51.

[4] L. Meal, Arson analysis by second derivative ultraviolet spectrometry, Anal. Chem. 58(4) (1986) 834-836.

[5] K.L. Bryce, I.C. Stone, K.E. Daugherty, Analysis of fire debris by nuclear magnetic resonance spectroscopy, Journal of Forensic Sciences 26(4) (1981) 678.

[6] J. Alexander, G. Mashak, N. Kapitan, J.A. Siegel, Fluorescence of petroleum products II: three dimensional fluorescence plots of gasoline, Journal of Forensic Sciences 32(1) (1987) 72.

[7] R.M. Balabin, R.Z. Safieva, E.I. Lomakina, Gasoline classification using near infrared (NIR) spectroscopy data: Comparison of multivariate techniques, Anal. Chim. Acta 671(1-2) (2010) 27-35.

[8] A.A.S. Sampat, B. Van Daelen, M. Lopatka, H. Mol, G. Van der Weg, G. Vivó-Truyols, M. Sjerps, P.J. Schoenmakers, A.C. Van Asten, Detection and Characterization of Ignitable Liquid Residues in Forensic Fire Debris Samples by Comprehensive Two-Dimensional Gas Chromatography, 5(3) (2018) 43.

[9] ASTM E1618-14, 2014, Standard Test Method for Ignitable Liquid Residues in Extracts from Fire Debris Samples by Gas Chromatography-Mass Spectrometry, in: A. International (Ed.) West Conshohocken, PA, 2014.

[10] E.E. Waddell, J.L. Frisch-Daiello, M.R. Williams, M.E. Sigman, Hierarchical Cluster Analysis of Ignitable Liquids Based on the Total Ion Spectrum, Journal of Forensic Sciences 59(5) (2014) 1198-1204.

[11] J.L. Frisch-Daiello, M.R. Williams, E.E. Waddell, M.E. Sigman, Application of self-organizing feature maps to analyze the relationships between ignitable liquids and selected mass spectral ions, Forensic Science International 236 (2014) 84-89.

[12] W.Y. Lu, J.G. Rankin, A. Bondra, C. Trader, A. Heeren, P.D. Harrington, Ignitable liquid identification using gas chromatography/mass spectrometry data by projected difference resolution mapping and fuzzy rule-building expert system classification, Forensic Science International 220(1-3) (2012) 210-218.

[13] T.-C. Jao, C.A. Passut, Handbook of Detergents, Part E: Applications, CRC Press, Boca Raton, FL, 2008.

[14] I. Barnett, M. Zhang, Discrimination of brands of gasoline by using DART-MS and chemometrics, Forensic Chemistry 10 (2018) 58-66.

[15] I. Barnett;, M. Zhang, Discrimination of Brands of Gasoline by Using DART-MS and Chemometrics, Forensic Chemistry 10 (2018) 58-66.

[16] J. McClelland, Rapid Arson Sample Analysis Using DART Mass Spectrometry, MFRC Final Report, Ames Laboratory–USDOE; Iowa State University, 2012, p. 24.

[17] E. Sisco, T.P. Forbes, Forensic applications of DART-MS: A review of recent literature, Forensic Chemistry 22 (2021) 100294.

[18] I. Barnett, F.C. Bailey, M. Zhang, Detection and Classification of Ignitable Liquid Residues in the Presence of Matrix Interferences by Using Direct Analysis in Real Time Mass Spectrometry, Journal of Forensic Sciences 64 (2019) 1486-1494.

[19] I.C. Willis, Z. Fan, J.T. Davidson, G.P. Jackson, Weathering of ignitable liquids at elevated temperatures: A thermodynamic model, based on laws of ideal solutions, to predict weathering in structure fires, Forensic Chemistry 18 (2020) 100215.

[20] T.J. Bruno, T.M. Lovestead, M.L. Huber, Prediction and Preliminary Standardization of Fire Debris Constituents with the Advanced Distillation Curve Method*, Journal of Forensic Sciences 56(s1) (2011) S192-S202.

[21] M.E. Sigman, M.R. Williams, Covariance Mapping in the Analysis of Ignitable Liquids by Gas Chromatography/Mass Spectrometry, Anal. Chem. 78(5) (2006) 1713-1718.

[22] ASTM E1618-19, 2019, Standard Test Method for Ignitable Liquid Residues in Extracts from Fire Debris Samples by Gas Chromatography-Mass Spectrometry, in: A. International (Ed.) West Conshohocken, PA, 2019.

[23] N.C.f.F. Science, Ignitable Liquids Reference Collection Database, University of Central Florida, 2001.

[24] W. Dong, J. Liang, I. Barnett, P.C. Kline, E. Altman, M. Zhang, The classification of Cannabis hemp cultivars by thermal desorption direct analysis in real time mass spectrometry (TD-DART-MS) with chemometrics, Anal Bioanal Chem 411 (2019) 8133-8142.

[25] U.S.F. Administration, Intentionally Set Fires, in: U.S.D.o.H. Security (Ed.) 2009.

[26] E. Stauffer, J.A. Dolan, R. Newman, Fire Debris Analysis, Academic Press2007.

[27] J.L. Berry, M.E. Gregg, A.A. Koepke, R. Newman, K.M. Jeerage, Concentration of ignitable liquid residue from simulated fire debris by dynamic vapor microextraction: Sensitivity to instrument settings and debris characteristics, Forensic Chemistry 35 (2023) 100511.

[28] É. Stauffer, J.J. Lentini, ASTM standards for fire debris analysis: a review, Forensic Science International 132(1) (2003) 63-67.

[29] A. E1412-19, Standard Practice for Separation of Ignitable Liquid Residues from Fire Debris Samples by Passive Headspace Concentration with Activated Charcoal, ASTM International, 2019.

[30] G. Fabrizi, M. Fioretti, L. Mainero Rocca, Occupational exposure to complex mixtures of volatile organic compounds in ambient air: desorption from activated charcoal using accelerated solvent extraction can replace carbon disulfide?, Analytical and Bioanalytical Chemistry 405(2) (2013) 961-976.

[31] W. Zhou, M.N. Wieczorek, H. Javanmardi, J. Pawliszyn, Direct solid-phase microextraction-mass spectrometry facilitates rapid analysis and green analytical chemistry, TrAC Trends in Analytical Chemistry 166 (2023) 117167.

[32] A. E2154-15a, Standard Practice for Separation and Concentration of Ignitable Liquid Residues from Fire Debris Samples by Passive Headspace Concentration with Solid Phase Microextraction (SPME), ASTM International, 2015.

[33] B.A. Capistran, Implementation of SPME and rapid GC–MS as a screening approach for forensic fire debris applications, Forensic Chemistry 38 (2024) 100562.

[34] I. Fettig, S. Krüger, J.H. Deubel, M. Werrel, T. Raspe, C. Piechotta, Evaluation of a Headspace Solid-Phase Microextraction Method for the Analysis of Ignitable Liquids in Fire Debris, Journal of Forensic Sciences 59(3) (2014) 743-749.

[35] K.G. Furton, J.R. Almirall, M. Bi, J. Wang, L. Wu, Application of solid-phase microextraction to the recovery of explosives and ignitable liquid residues from forensic specimens, Journal of Chromatography A 885(1) (2000) 419-432.

[36] S. Perna, B.M. Dedicatoria, N.S. Chong, M. Zhang, GC/MS and DART-MS as complementary methods for investigating the effects of weathering on chemical profiles of ignitable liquids: A case study for paint thinner, Forensic Chemistry 33 (2023) 100478.

[37] W. Romão, L.V. Tose, B.G. Vaz, S.G. Sama, R. Lobinski, P. Giusti, H. Carrier, B. Bouyssiere, Petroleomics by Direct Analysis in Real Time-Mass Spectrometry, Journal of the American Society for Mass Spectrometry 27(1) (2016) 182-185.

[38] A. Khaled, J.R. Belinato, J. Pawliszyn, Rapid and high-throughput screening of multi-residue pharmaceutical drugs in bovine tissue using solid phase microextraction and direct analysis in real time-tandem mass spectrometry (SPME-DART-MS/MS), Talanta 217 (2020) 121095.

[39] R.V. Emmons, W. Fatigante, A.A. Olomukoro, B. Musselman, E. Gionfriddo, Rapid Screening and Quantification of PFAS Enabled by SPME-DART-MS, Journal of the American Society for Mass Spectrometry 34(9) (2023) 1890-1897.

[40] J.A. Jastrzembski, G.L. Sacks, Solid Phase Mesh Enhanced Sorption from Headspace (SPMESH) Coupled to DART-MS for Rapid Quantification of Trace-Level Volatiles, Analytical chemistry 88(17) (2016) 8617-8623.

[41] I. Barnett, F.C. Bailey, M. Zhang, Detection and Classification of Ignitable Liquid Residues in the Presence of Matrix Interferences by Using Direct Analysis in Real Time Mass Spectrometry, Journal of Forensic Sciences 64(5) (2019) 1486-1494.

[42] Ignitable Liquid Reference Collection (ILRC). .

[43] M. Sigman, Final Summary Report for Substrate Pyrolysis Database Expansion, Evaluation, and Use, National Criminal Justice Reference Service, 2018.

[44] PubChem Compound Summary for CID 31292, Octadecanamide. , National Center for Biotechnology Information

[45] M. Beaumesnil, A.L. Mendes Siqueira, M. Hubert-Roux, C. Loutelier-Bourhis, C. Afonso, A. Racaud, Y. Bai, High-performance thin-layer chromatography with atmospheric solids analysis probe mass spectrometry for analysis of gasoline polymeric additives, Rapid Communications in Mass Spectrometry 34(S2) (2020) e8755.

[46] P. Zuo, W. Shen, Identification of nitrogen-polyaromatic compounds in asphaltene from co-processing of coal and petroleum residue using chromatography with mass spectrometry, International Journal of Coal Science & Technology 4(3) (2017) 281-299.

[47] S. Maity, 2 - Applications of selected response surface design of experiments and advanced control charts in textile engineering, in: R. Chattopadhyay, S.K. Sinha, M.L. Regar (Eds.), Textile Calculation, Woodhead Publishing2023, pp. 13-55.

[48] B.C. Reaser, B.W. Wright, R.E. Synovec, Using Receiver Operating Characteristic Curves To Optimize Discovery-Based Software with Comprehensive Two-Dimensional Gas Chromatography with Time-of-Flight Mass Spectrometry, Analytical chemistry 89(6) (2017) 3606-3612.

[49] K. Hajian-Tilaki, Receiver Operating Characteristic (ROC) Curve Analysis for Medical Diagnostic Test Evaluation, Caspian J Intern Med 4(2) (2013) 627-35.

[50] A. E1618-19, Standard Test Method for Ignitable Liquid Residues in Extracts from Fire Debris Samples by Gas Chromatography-Mass Spectrometry, ASTM International, 2019.

[51] M.N. Torres, J.R. Almirall, Evaluation of capillary microextraction of volatiles (CMV) coupled to a person-portable gas chromatograph mass spectrometer (GC–MS) for the analysis of gasoline residues, Forensic Chemistry 27 (2022) 100397.